CRISS
(Consortium for Research In Space Systems)

BITS Pilani, Pilani Campus

CRISS

Consortium for Research In Space System

Team Lead: Swapnil Padhi swapnil18800@gmail.com

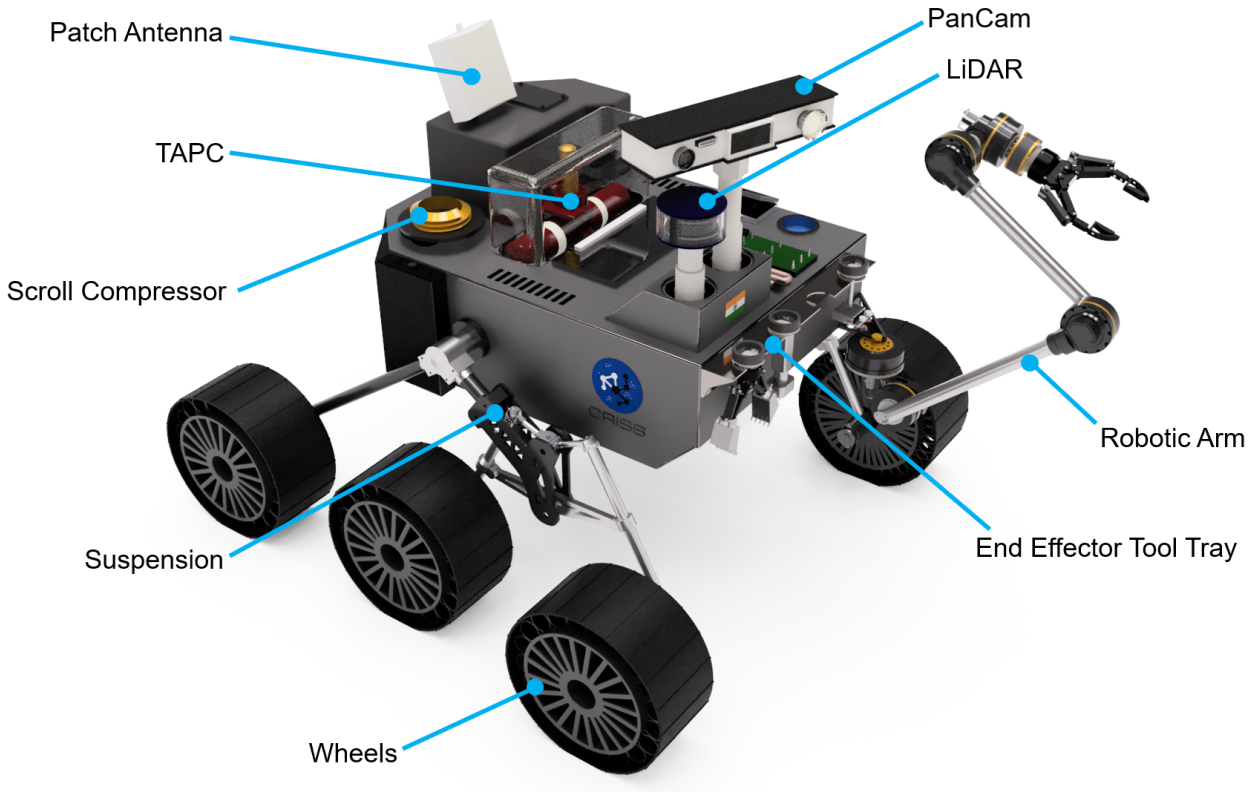
Patch Antenna
PanCam
LiDAR
TAPC
Scroll Compressor
Robotic Arm
End Effector Tool Tray
Suspension
Wheels

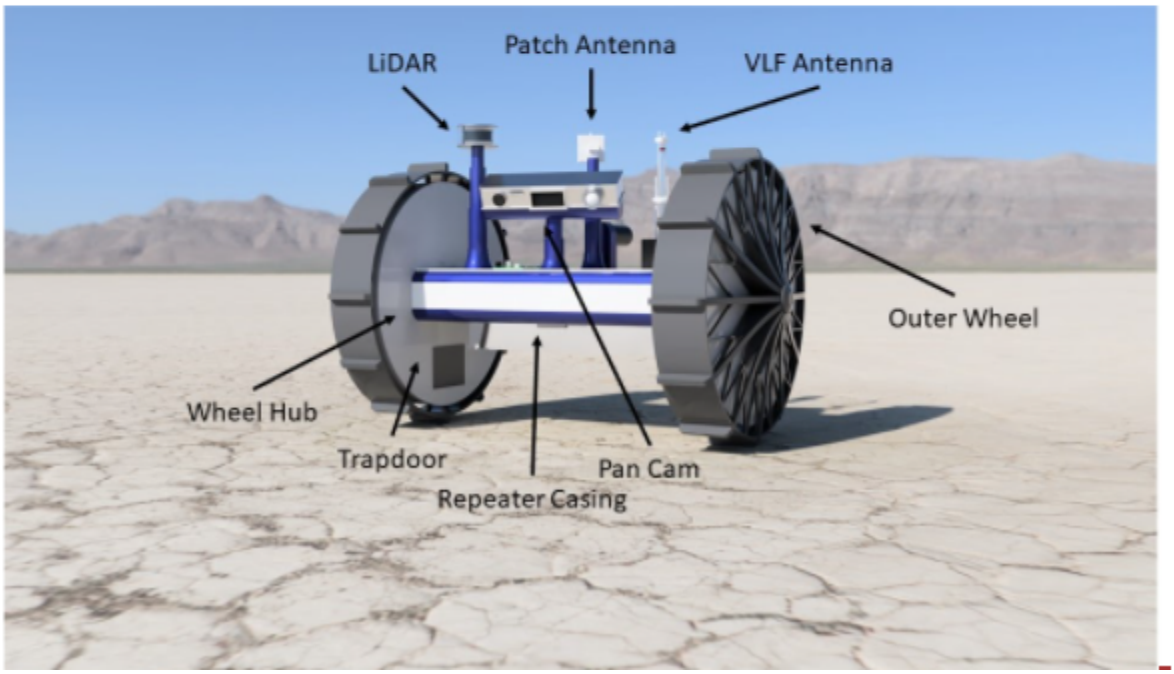
LiDAR
Patch Antenna
VLF Antenna
Outer Wheel
Wheel Hub
Trapdoor
Pan Cam
Repeater Casing

ABSTRACT

Space exploration has taken an interesting turn, with researchers finding interest in human settlements on other planets, Mars proves to be a constant source of buzz, excitement and speculation. It provides hope for human settlements and the exploration of 'Martian Lava Tubes' strengthens our beliefs further. Satellites provide images of skylight entrances to these tubes, however in depth research about them is not yet exhausted. Keeping these factors in mind our team, CRISS has written an in-depth exploration mission report to further study and analyse the conditions of these unknown sites. In our report, we propose detailed mechanical designs, well thought out electrical systems, science experiments for research and study and efficient software to integrate the systems. We have taken a mission based approach, considered the various complexities of the harsh Martian environment and provided innovative and novel solutions to them, backed with current technical advancements and keeping in mind the future scope.

CONSIDERATIONS & REQUIREMENTS

The following assumptions are considered while traversing the lava tubes:

The dimensions of the tube are over 50m in width and situated 15m below the ground level protected from a major portion of the rough martian surface conditions such as dust storms, radiation etc. The terrain of the lava tubes is considered to be evenly traversable with the exception of debris and other abnormal landscape encountered. A single rover consisting of conjoined scout bots and a science bot is deployed along with the configured communication equipment such as a parabolic antenna, a leaky feeder, and the required transceiver. Temperatures are assumed to vary from -70 to +25 °C and we have designed the rover to be stable around a fixed temperature. This assumption is needed to avoid issues caused due to differences in rates of expansion or contraction of different materials due to fluctuating temperatures. We have also taken into account the Triboelectric effect in which due to dryness, charge buildup is common. A discharge mechanism must be put in place to avoid uncontrolled discharging [2.12]. Discharge points were made using needles to discharge through, and a few micrograms of Americium-241, whose emissions will ionize the air and allow for conduction through it [2.13]. We have finally assumed that we have sufficient sensors to map the lava tube, gradient of the terrain, images and videos, and store and process a large amount of data.

MISSION PLAN

The main and trivial objective of our mission is to explore the martian tubes, thus the further distribution of tasks are:

Objectives	**Pre-requisites**
Traversing and Mapping the Lava tubes	Keeping the rovers powered up for > 10 hours
Identifying Regions of Interests	Building a robust rover capable to traverse the martian lava tubes
Investigate life forms and geochemistry	Design Science mechanism for the rovers
Capturing Images/Videos of the lava tube	Building the Communication network so that the rovers stay in contact with each other and base station at all times.

Keeping these objectives in mind, we designed one base system that can be lowered in the martian lava tube through the skylight entrance termed *Base Skylight*. After reaching the surface of the lava tube, the base system will detach into a main science rover and 4 scout bots.

The Science rover is big and houses a lot of science equipment for detailed testing of the region, whereas the scout bots are smaller but quicker and will mostly be used for navigating and mapping deep in the lava tube and conducting some scientific tests. The tasks of the different rovers have been depicted in the above image.

Scout Bot Architecture:
MECHANICAL

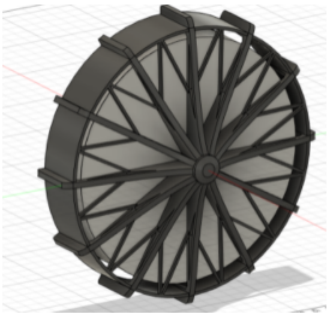
Wheel Mesh Design

Mobility: The scout bot uses a two-wheel system. The wheels are large (0.8 m in diameter, 0.15m in thickness) and provide extra traction needed for a relatively high top speed (1 m/s). The larger diameter of the wheels also ensures the bot can traverse obstacles about 1.4 times its radius with relative independence. This also enables the rover to maintain its mobility in a variety of positions, as well as giving it high efficiency over the predicted relative flat ground of the Lava Tube. This unique inter-scout bot docking further enhances the obstacle clearance capabilities of the Scout bot. For traversability of extreme slopes, the docking mechanism can be outfitted with a cable used for rappelling down rocky faces. Multiobjective optimization was performed to arrive at a suitable wheel diameter and width and power consumption was minimized while wheel traction and the ability to climb steep slopes was maximized.

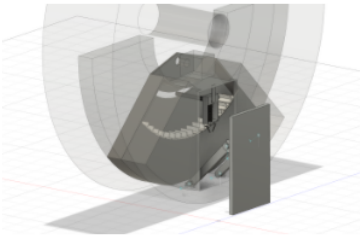
Science Hub Gantry System

Science Hub Mechanism: Taking advantage of the bot's mobility systems, the wheels are covered in a mesh-like structure, enabling us to use the immobile inner hub of the chassis for other tasks. This helps us mount and take in more soil testing equipment along on the scout bot, which can be deployed by a compact 2-bar linkage that takes the various onboard sensors close to the ground to perform the required analysis. Further, a swab soil-collection system is also incorporated on the other side by an intricate design, which enables us to store up to 30 samples of soil, which can be used for further testing after the return of the scout bot.

Docking Mechanism: When travelling over extremely undulating terrain, the two scout bots get connected to each other by means of a latch mechanism. This helps in giving extra power and traction to the system and to successfully traverse the lava tube. To decouple, a linear actuator is used for the latch.

Materials: We used Aluminium, Titanium Grade V, and Aerogel in our scout bot chassis. Due to its strength and lightweight properties, Aluminium was the obvious choice to use for the chassis. Titanium Grade V, due to its immense strength, gives chassis crucial support. To keep the chassis warm and to prevent heat leakage, Aerogel was used to insulate the chassis.

Repeater Dropping Mechanism: To ensure continuous connection, cube-shaped repeaters placed below the chassis are dropped as the scout bot travels deeper into the lava tube. This is achieved by storing about 30 repeaters in a 3x10 array below the chassis, which can be controllably deployed via a conveyor belt system at regular intervals.

Science Bot Architecture:

Wheels: Due to the similarities in the geological process that forms both terrestrial and Martian lava tubes, we expect the terrain to consist of flat hard rock. The science bot wheels are designed to find purchase in this terrain with the help of grousers. The wheel is also designed to be slightly flexible. The ring-shaped spokes and wheel rim flex to ensure contact of multiple grousers with the ground at a time increasing grip. The width and diameter of the wheel were obtained using multiobjective optimization with goals including the reduction of the power consumption and maximization of traction and slope traversability.

The wheel is made from Al 6061-T6 except for the grousers, which are made from Al 7075 -T7351. Al 6061-T6 is used in the majority of the wheel due to its relatively high strength to weight, corrosion resistance, and ease of manufacturing. As per our simulations, Al 6061 possesses enough flexibility for use in the rim and wheel spokes. The grousers were chosen to be made using Al 7000 series due to their superior hardness as compared to the 6000 series.
The motors used have a torque requirement of 22.60 Nm at 25rpm and the maximum speed is 0.5 m/s The motors chosen are Avior Systems D-N100R-02 motors. The motor is rated for space use, uses dry lubricant, and possesses one mode of redundancy.

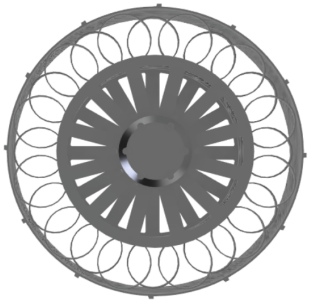

Scout wheel Side View

Scout wheel Isometric View

Suspension: Since the rover is expected to encounter and traverse through harsh and unexplored terrain of the Martian lava tubes, the suspension had to be designed with great care. At the heart of our suspension lies the reliable and sturdy '6 wheeled Rocker-bogie suspension system'. A conventional rocker-bogie consists of a pivoted bogie at the front and a rocker at the rear to ensure uniform contact with the ground and great traction even while climbing large vertical obstacles.The material used is titanium alloy.

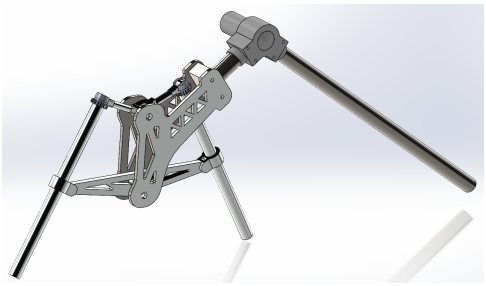

Our front rocker has been modified using a set of 4-bar-linkages popularly known as Chebyshev's double lambda mechanism. This allows linear motion of the front rocker instead of a circular motion while keeping the pivoting torque from an obstacle to a minimum. It also lowers the effective pivot point while keeping the ground clearance unaffected. The motion

analysis results show that our modified rocker-bogie is considerably more stable, faster, and can climb over more rugged terrain as compared to the conventional rocker-bogie design.

Chassis: A low mass chassis would enable the rover to survive rough terrain without damaging the suspension as well as increasing the power efficiency of the driving motors. Hence, a space frame chassis design with diagonal tubes was used to provide rigidity in all directions. The frame has been made out of Grade 5 Titanium alloy (Ti 6Al-4V), inspired by the halo protection device used in Formula 1 cars. This alloy is known for its high strength and low weight. Cylindrical tubes were used because of their ability to withstand torsional forces.

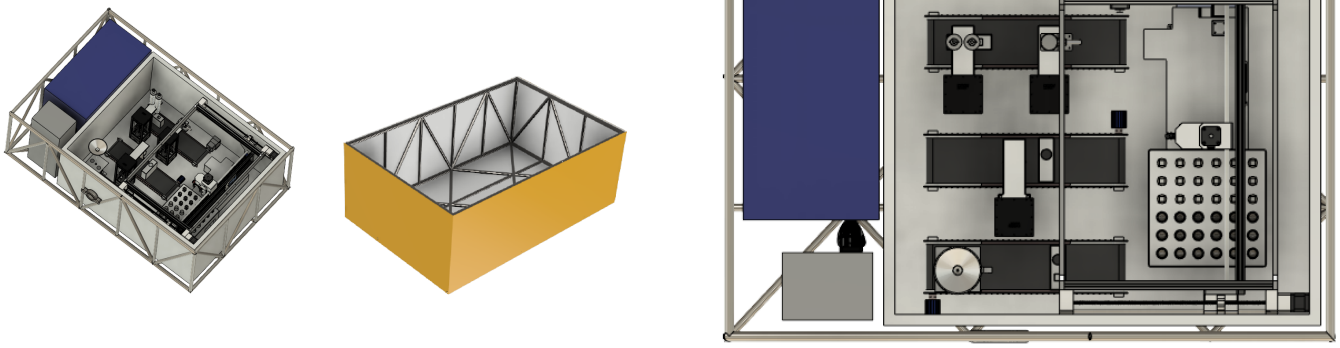

(a) (b)

Figure (a) depicts the contents of the chassis. Figure (b) depicts the empty chassis, it is coated by gold

Honeycomb sheets made out of aerospace-grade Aluminium alloy 7075 were used to seal the chassis. This alloy offers high machinability as well as the optimum strength-to-weight ratio. The sheet is lined with 1 to 3 cm thick silica fibre-doped cross-linked aerogel that has an extremely low thermal conduction but can withstand the expected load and bends. This minimises heat loss from the chassis. Hatches have been carved into the chassis for greater modularity of the science-testing module. These hatches have been lined with fluorosilicone rubber that has a lower operating temperature bound of 193 K, suitable for the Martian environment.

Science Instrument Payload

Holographic spectrometer

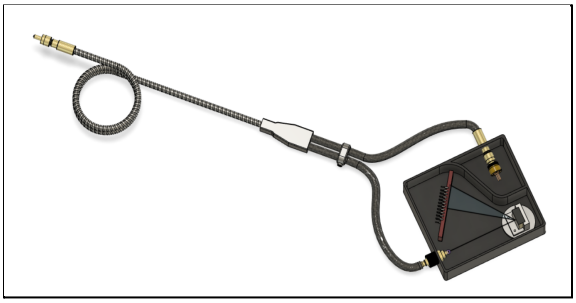

Holographic spectrometry is a novel method of a non-invasive form of spectroscopy, located on scout bot that uses a holographic diffraction grating to produce spectra of light reflected off the soil or rock sample in consideration. After which, the reflected light passes through a reflective optic fiber probe and cable placed along the mechanical arm and post reflection off the 600g/mm grating. A linear CCD array later analyzes The resultant spectrum. This analog output is then processed to

identify the minerals present with the help of an FPGA circuit that converts the analog output of the CCD array to digital data for a software system to develop graphical results.

Raman Spectrometer

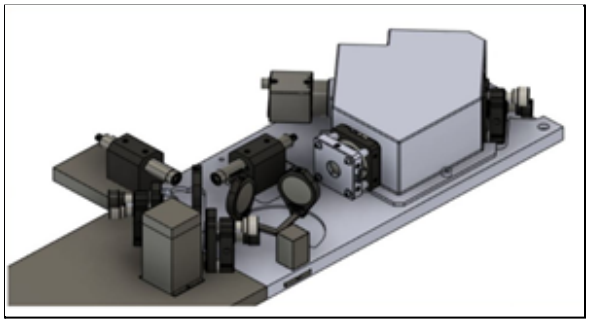

A custom multi-laser Raman spectrometer detects key biomarkers and minerals such as nucleic and amino acids, lipids, saccharides, and minerals. The instrument will be placed inside the science bot. The shift in wavelength of the Raman scattered particles generates a fingerprint by which molecules can be identified. Raman Spectroscopy was incorporated on the rover as it is a fast technique that requires no sample preparation and can uniquely identify different biomarker compounds. A multi-laser system (532nm and 785 nm) is used to obtain the Raman spectra of the sample at both wavelengths and detect the maximum number of biomarkers. The output of the CMOS detector is used by an onboard processor to produce graphs and identify the biomarkers.

Mini-Thermal Emission Spectrometer + Panoramic Camera Assembly

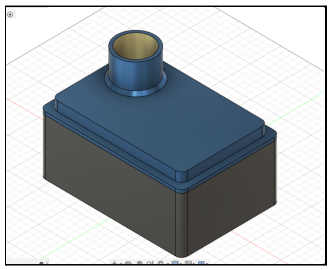

This assembly, mounted on both bots, serves to map out the mineralogical composition of the soil or rock and water vapor abundance in the surrounding terrain of the rover. The camera helps in detecting goethite formation and surface oxidation rate. Mini-TES observes the scene through a periscope assembly shared with the camera. The panoramic camera provides color stereo pictures of terrain with the help of a focusing mechanism to capture images at a distance and multispectral filters, while Mini-TES provides remotely sensed point discrimination of mineralogical composition of surrounding in the camera's Field of view. The optical path follows through a Cassegrain telescope, Michelson mirror, and an imaging parabolic mirror before culminating in a detector assembly. The output interferogram of the DTGS detector is converted into 16-bit spectra via Fast Fourier Transform (FFT). A CMOS sensor captures the light rays from the multispectral filters in the camera, and the average spectral information is inferred.

Alpha Particle X-Ray Spectrometer (APXS)

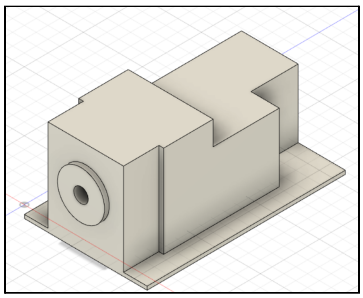

Alpha Particle X-Ray Spectrometer measures the elemental composition of soil surfaces on Mars. It is placed inside the conveyor belt on the Science bot and is held vertically by a linear actuator. The sample is irradiated with alpha particles and X-rays emitted from the radioactive decay of Curium-244. The alpha particles and X-rays knock electrons off the orbit of elements present in the samples and emit energy in the form of X-rays detected by the silicon sensor. The energies of these emitted X-rays are characteristic of specific elements by Particle Induced X-Ray Fluorescence and X-Ray Fluorescence and help in their detection. The output from this technique will be spectra of elements plotted on graphs with energy (keV) against the count rate, which will then be compared to their standard measurements.

ATP Bioluminescence Test

Placed in the science bot, this technique detects the presence of ATP, which indicates biomass, metabolism, and life's presence in the lava cave. ATP swabs are used to collect a soil sample from the floor and walls of the lava tubes. After soil collection, the swab is dropped into ATP testing assembly containing luciferin-luciferase enzyme. The luciferin-luciferase reagent reacts with ATP residue-emitting bioluminescence which is then measured by the luminometer. It measures this weak light emission through a photomultiplier tube and displays results in Relative Light Unit (RLU) values. These values for each site, along with its coordinates, are sent to the onboard computer.

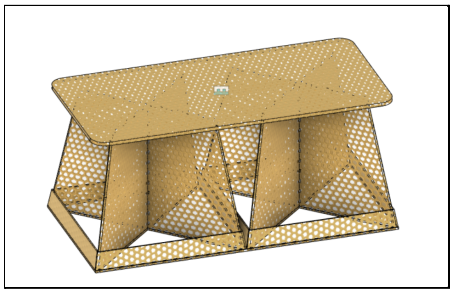

Ground Penetrating Radar

Located on Science bot, it investigates the distribution and state of subsurface water, brine, and surface's geographic profile. The GPR system consists of the antenna assembly and the electrical unit. The antenna assembly consists of two antennas (cross structure), transmitting and receiving antenna arranged together to one baseplate. The electrical unit generates a sinusoidal wave, in the frequency range between 500MHz and 3GHz. A part of the wave is scattered to the antenna assembly whenever it encounters the interface of two different mediums. All the reflected waves superimpose at the receiver, returning the value indicating the strength of the received signal. The data processing of GPR will be done in the base station. The samples will undergo laboratory characterization for electromagnetic properties and numerically simulated radar grams are obtained.

Field Microscope

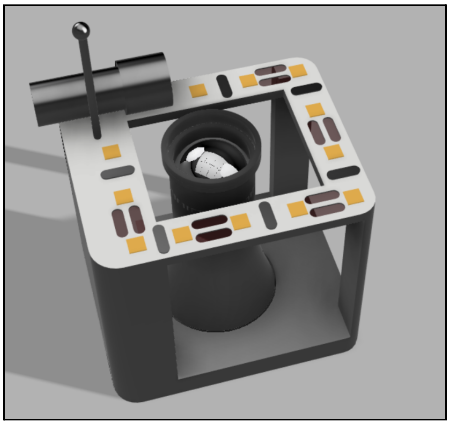

Located on the arm of the Science bot, the field microscope provides a magnified fine-scale image of the Martian surface, which is used to determine if water existed on Mars. It is also used to study the texture of the Martian surface, which is compared to existing standards. Some nanofossils can be identified in this process. This instrument uses a fixed-focus microscope and camera to acquire images at a spatial resolution of 30 microns/pixel over a broad spectral range (400 - 700 nm). CCD is used for image storage during readout. Integration of another image begins once the readout of an image is complete. Deep learning algorithms are employed to process and identify nanofossils and signs of water on ancient Mars. The scout bot also houses a mini-digital microscope for analysis of surface features.

Atmospheric and Soil Sensors

The Scout and Science bot consists of a suite of sensors for atmospheric and soil analysis and determining if the environmental conditions are conducive for life. Gaseous sensors onboard include carbon dioxide, methane, carbon monoxide, volatile organic compounds, oxygen, ammonia, nitrogenous gases, UV, and ionizing radiation. Soil sensor involves one probe to measure its pH, electrical conductivity, and NPK concentration

Thermo-Acoustic Power Converter (TAPC)

Multiple options were considered and finally, TAPC was selected, details of which can be found in Appendix B.1.2. TAPC is a radioactive electric power generator that operates on Stirling thermodynamic cycle. It is powered by 2 general-purpose heat source modules (GPHS).Each GPHS module is fueled by plutonium-238 oxide and is capable of providing around 250 Watt of thermal energy for a long period of time and weighs around 1.44 kg. TAPC has dimensions of 417.6 mm × 247.7 mm × 142 mm, it has an efficiency of 25.83% which when converted to absolute numbers, provides up to 129 Watts of AC electrical power at the beginning of life. It can continuously provide power for up to 17 years. TAPC's Stirling engine unit weighs around 15 kg and its Converter unit weighs around 6.42 kg which comes to a total of 21.42 kg.

Thermo-Acoustic Power Converter (TAPC) will be used to recharge the battery pack on the science rover; it has a specific electrical power of 8.6 Watt per kg and it provides 130 Watt of electrical power with an output RMS voltage of 86.9 Volts and output RMS current of 1.8 amperes. Heat rejected by the TAPC unit is used for thermal management of the rover to keep the components warm.[2.23]

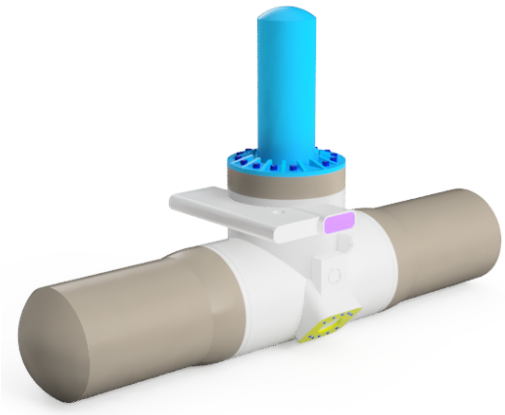

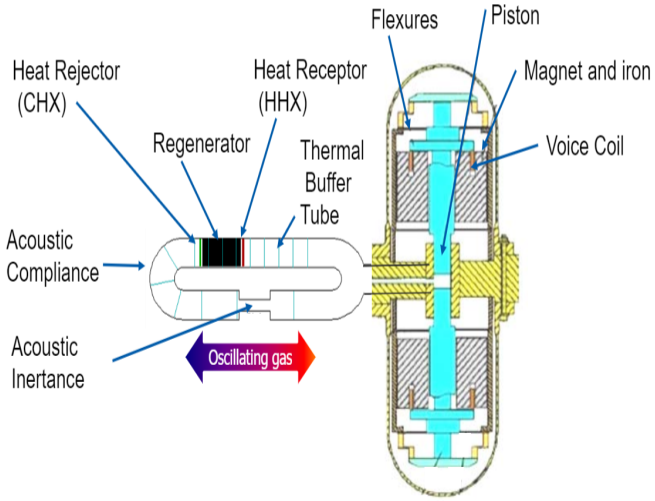

(a) Isometric-view
(b) cross-section view

Thermo-Acoustic Power Generator

Thermal management system

A thermoacoustic power converter releases heat of around 350 Watts. This heat will be used for warming the components in the chassis. TAPC is enclosed in a shell and the walls of the TAPC compartment are lined with aerogel. The chassis requires around 60 watts of heat to maintain a constant temperature of 25 degree celsius. The thickness of Aerogel at the walls in contact with the chassis is 20 mm.

ELECTRICAL

Semiconductors

Gallium Nitride (GaN) based electronics were used because of the wide operable temperature range [2.1] and lowered susceptibility to dust [2.2] and radiation [2.3]. GaN-based devices outperform modern radiation-hardened Silicon-based MOSFETS because of the strong wurtzite crystal lattice [2.4]. The various advantages of using GaN-based devices in our circuits are addressed in the respective sections in the respective contexts. The circuits designed are further enclosed in a protective layer of epoxy resin matrices which uses CNTs and Tungsten nanoparticles as fillers. [2.5].

Embedded Systems

The overview of the system can be found in B.2.1. The drive systems of both bots employ the differential drive method for steering. Furthermore, a fuzzy PID based algorithm is used for the self-balancing of the 2-wheeled scout bots. [2.14].

Digital Equipment

GaNFETs provide lowered off-currents and improved on-currents, thereby providing higher performance than their radiation-hardened silicon counterparts [2.9]. All embedded systems were implemented using the appropriate specialized and optimized GaN-based ICs and PCBs. The powerful onboard computer (whose specifications can be found in B.2.3) is used to execute all heavy-duty algorithms on both bots. For the collection and storage of bulky data, a 4 TB memory device was used. A system with commercial off-the-shelf unhardened memory units coupled with sufficient countermeasures was used over rad-hard memory because of performance and cost advantages. Over and above the previously mentioned countermeasures, TMR via three identical memory units was used to mitigate SEFI. Similarly, Hamming codes were employed for the mitigation of SEU [2.6].

Motors

Modified versions of the listed off-the-shelf motors were used to cope with the Martian conditions (Refer to B.2.3). Both brushed and brushless DC motors were used, along with the appropriate motor drivers, optical encoders and microcontrollers.

1. Outgassing was combated by using Teflon-based stators, rotors, end caps, and screws [2.15]. Furthermore, motors were thoroughly vacuum baked before operation.
2. A Solid lubricant with low vapour pressure, Molybdenum disulfide, was used. Wet lubricants were refrained from using as they are subjected to evaporation due to their high vapour pressure and have poor temperature viscosity characteristics [2.16].
3. Brushes made up of silver graphite with 15% Molybdenum disulfide are used. It prevents cold welding and wear-and-tear of brushes due to low water vapour and oxygen content in the atmosphere [2.17].
4. Demagnetization in extreme temperatures was combated by using Neodymium-Iron-Boron based permanent magnet motors.
5. Dust prevention is done by carefully sealing the opening of motors.

Power architecture

The system overview can be found in Appendix B.1.1. Sion's Licerion Pouch Cells numbered BX-6S2P-24-40 were used for powering the rovers[2.27]. Each pack is 6S2P and comes with a nominal voltage of 22.9 V and its current capacity is 40 Ah and has a maximum continuous discharge rating of 80A. Each pack has 917Wh of energy capacity. It has inbuilt safety features like over-charge, over-discharge, over-temperature and over-current protection. Each module is also equipped with fuses and switches. 8 such battery packs were used in the science rover and 6 such battery packs in the scout rover. The battery pack is encased in the "space suit" lining design to protect against debris and offer thermal and radiation protection, in addition to what was mentioned earlier in the 'Semiconductors' section.

In the science rover at a time a single battery pack will power the entire rover once the battery pack discharges; the next battery pack will be used to power the rover. A thermoacoustic power converter will be used to recharge the discharged batteries. AC-DC power converter by XP power with model number ASB110PS24 which boasts up to 91% efficiency will be used to convert AC output from thermoacoustic power converter to DC output of 24 V[2.28]. On the scout rover, all six battery packs will be connected in parallel.

A power distribution board(which has the same architecture in both science rover and scout rover) will be connected to the battery pack which contains a set of DC-DC converters and safety circuits for overcurrent protection. Monolithic GaN-based power converters will be used for the high switching frequencies, higher efficiency, overall smaller size of the systems and hence lowered die sizes, lowered parasitic inductances, and easier thermal management [2.7].

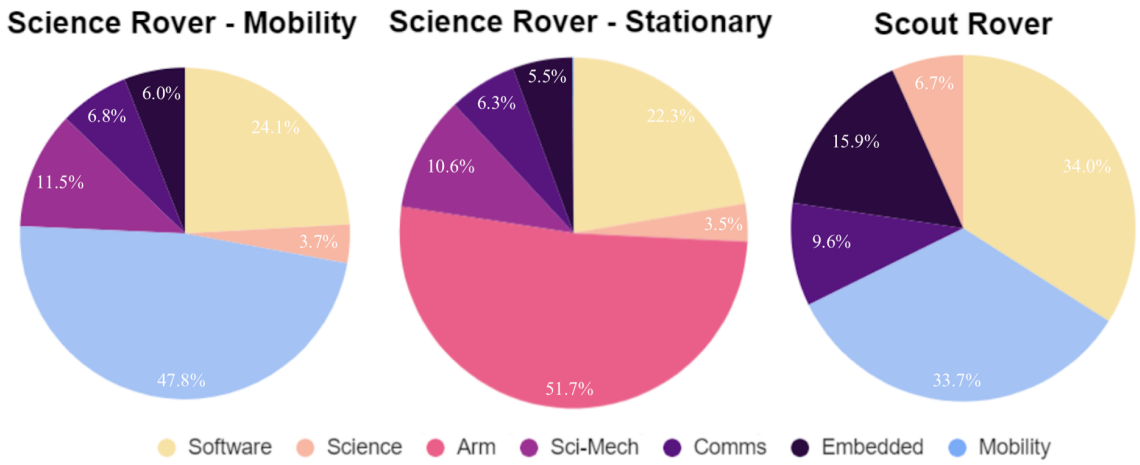

Fig. 1.2 Breakdown of the power consumption in the Science and Scout Bots

Detailed breakdown of power consumption can be found in B.1.3.

Communication Systems

The communication architecture proposed in this report involves a primary 900 MHz link coupled with the functionality of a VLF link as well. We propose the demarcation of the mission terrain into two regions, a high data rate region (characterized by a mesh network of repeaters yielding a high data rate link to the base station, abbreviated as HD region), and a low data rate region (characterised by a low data rate link over VLF to the base station, abbreviated as LD region). The demarcation is brought about as the bot is continuously monitoring the quality of the link. Once a certain minimum threshold is breached, the bot moves into VLF communication and is thus in the LD region. Apart from the links from the bots to the base station, a high-speed link in the 900 MHz band is maintained between the two scout bots (link margin calculations for all these links are attached in Appendix B.3.2). A brief description of the hardware used is provided below (the whole architecture in the form of a block diagram is provided in Appendix B.3.1). The team assumes the availability of the entire spectral range during our mission.

Components at Base Station: The base station comprises a 433 MHz communication setup. While the main communication in the lava tube happens over 900 MHz channels, 433 MHz was chosen for the base-skylight link due to its low power consumption at a similar bandwidth. The setup consists of a parabolic dish antenna coupled with custom-designed transceivers which support the data rates comparable to the 900 MHz spectrum.

Components at Skylight Entrance: To enable communication between the base station and rovers inside the lava caves a communications node will be present on the Martian surface near the skylight entrance. This will consist of a 433 MHz and VLF communications set up along with a 900 Mhz radiating cable.

a. VLF Antenna- The VLF (Very Low Frequency, 3-30 kHz) antenna in our system is an ultra-low-loss, rod shaped-piezoelectric material based electric dipole driven at acoustic resonance. An oscillating electric voltage is applied to the bottom of the rod to make it vibrate. This mechanical stress triggers an oscillating electric current whose electromagnetic energy then gets emitted as VLF radiation. Utilizing piezoelectricity as the radiating element allows us to repeatedly switch the wavelength which gives a better system bandwidth [2.18].
b. Leaky Feeder Cable - A 900 MHz leaky feeder cable will be suspended from the skylight entrance. The cable is "leaky" in that it has slots in its outer conductor to allow the radio signals to leak into or out of the cable thus functioning as an extended antenna. The function of the cable is to receive data from the near scout or science bots/repeaters and route the data to the 433MHz link which in turn relays it to the base station. The cable will have a radiating slot suspended near the centre of the lava cave so as to offer maximum range by eliminating possibilities of line-of-sight obstructions [2.19].
c. 433 MHz Parabolic Dish Antenna - This antenna is present just outside the skylight entrance and provides the final leg of communication from the skylight to the base station.

Repeaters: These are cube-shaped modules with a side length of 5 cm containing a 900 MHz patch antennae (~ 10 dB gain) on all their faces. On-Board circuitry allows for the repeater to find the most optimal face (that which is devoid of contact with the ground, facing a conducive direction for transmission, etc.) for use. The repeaters are tasked with amplifying the signal received and transmitting it along with the repeater network so as to increase the range of high-speed communication (the high data rate region is characterised by their presence).

Rover Components:

a. 900 MHz Patch Antenna - This patch antenna will be mounted on a rotating frame to provide a directional link to other nodes in the cave. Periodic structures, namely metasurfaces are used as a superstrate above the antenna, to increase the gain to 15 dB.
b. On-Board VLF Antenna - This antenna facilitates a link that will be used for transmission when rovers move into the Low Data Rate region (present only on the scout bots).

GaN on SiC HEMT based RF Power Amplifiers were used in the communication systems. GaN technology offers increased linearity and supports the required output power of 20-30 W comfortably [2.10]. The PAs used are similar to those offered by [2.11].

Protocols, Networking & Data Handling - Communication in a cave environment is susceptible to multipath fading and inter-symbol-interference, hence the OFDMA scheme (OFDM for multiple users) will be used to diminish the effect of multipath [2.20]. In the 900 MHz Mesh Network, repeaters/bots can talk to each other directly as long as they are within the radio range of each other. If they are beyond each other's radio range then the message will travel through other nodes, according to a path which the network will establish based upon efficiency.

To find a mesh route, a route request broadcast will be sent out by the scout/science bots. Other nodes will receive this broadcast and see if they know the destination. They will forward the route request if they do not know the destination, with the incremented path cost. If they do know the destination, they will send a reply to the originator. The reply message contains the total length of the routing path to the destination which makes it possible for the originator to determine which route is the best when multiple route replies are received. In this network, when there is more than one way to relay a message the most cost-effective route is selected. This means that if a repeater in a route path fails due to reasons such as exhaustion of its battery, the originator node will find an alternative router to relay the message to the destination node. The devices will transmit over different non-overlapping channels to minimise interference[2.21].

Inside the rovers, OBC will be responsible for receiving data from different parts of the rover, applying the necessary communication/mesh networking protocols and scheduling the packets according to their priority before sending them to other nodes. A comprehensive block diagram of the system architecture can be found in Appendix B.2.1.

Robotic Arm

The robotic arm is a state-of-the-art, modular, 5 Degree of freedom robotic manipulator used to perform tasks like drilling, collecting soil, etc. to facilitate the study of the Martian environment. This robotic arm features detachable end effectors enabling us to perform a wide range of tasks.

After exhaustive workspace calculations and placement of instruments on the chassis, the arm is placed on the front face of the chassis to allow for easy maneuverability and seamless retraction when not in use. This makes the arm compact for transportation purposes and prevents damage as well.

(a)  (b) 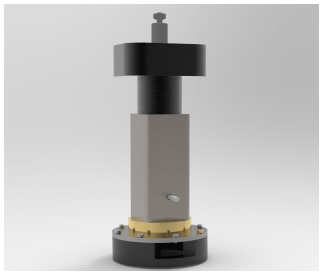

(c) 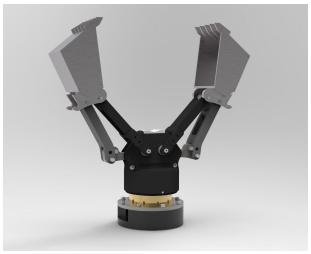 (d) 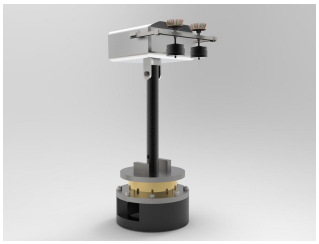

End effectors (a) Gripper (b) Drill (c) Scoop (d) Dust Collector

The docking mechanism is developed for easy dynamic attachment and detachment of end effectors (refer A.3.1 for tool tray) . It incorporates a screw and 2 metal balls to provide a vibration-free attachment [1]. It also accounts for the transmission of power and controls of the end effectors.

Gripper: The gripper is based on the 4 bar mechanism [2] and is used to hold swabs for soil collection, hold the 5 in 1 probe, and spectrometer for performing science tasks. It can also be used for holding tools to perform repairs on the rover.

Drill: The drilling system uses a crank mechanism to jackhammer a diamond drill bit [3] rotating at 100 rpm [4] into the hard Martian surface. The rock and dust particles generated are collected and used for scientific analysis.

Scoop: The scoop is also based on the bar mechanism with claws[5] and is used to directly collect soil from the ground. It can also be utilized for moving rocks upto 3kg from one place to another.

Dust Collector: The dust collector is used for collecting the dust of the rock particles or the leftover loose soil. Two brushes are rotated with motors and the particles are collected in the collector tray attached which is used for testing.

The 3 main joints of the arm use highly reliable Maxon DC motors [6] with a primary 3 -Stage reduction from a planetary gearhead and a secondary customized harmonic gearbox (refer A.3.4) which reduces the rpm and gives the necessary torques (refer A.3.2 for torque calculations) to perform the actuations.

The links of the arm are made up of a Titanium alloy and have a circular cross section. Structural Analysis (refer A.3.3) suggests that the Factor of Safety of both the links are 41 and 44 respectively which should be fairly safe to operate in the Martian environment.

The arm is designed to facilitate easy retraction (A.3.5) to prevent damages, and make the arm compact for transportation. The arm is mounted on the front face of the chassis to enable this retraction.

Soil quantity control:

Filtered soil is poured into the upper funnel which is connected right below the science module lid. The funnel contains 3 electrically actuated aperture doors at the opening of the funnel, middle part and the tube outlet. These doors are strategically timed and opened/closed to pour out a specific volume of soil. The soil transfers through the tube which connects directly to the cuvette and test-tube holder and prevents soil spillage even while the chassis is tilted. Final outlet can shift between cuvette and test tubes using a linear actuator. Also consists of UV light radiators that are switched on to prevent cross contamination.

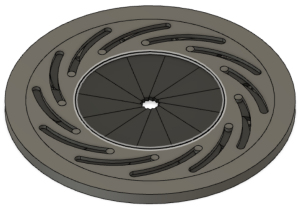

Aperture door

Soil quantity control unit

Internal Science mechanism:

The science module is of dimensions 964 mm × 810 mm × 425 mm. The test tubes are used for storing samples and for the APXS test, while cuvettes are used for the Raman spectroscopy test. An estimate of 15 sites was decided and hence 18 test tubes and 18 cuvettes were planned to be stored, and not be reused. A gantry system is used for internal transportation along with 3 conveyor belts. Conveyors 1, 2 and 3 move the cuvettes/test tubes to and from the soil filtration, the APXS test, and the lid placing mechanism respectively. The basic sequence of events is as follows:

Step 1: The test tubes and the cuvettes are initially placed in a storage array. Using a gantry system they are moved to conveyor 1. Conveyor 1 moves them to the soil collection area,

Step 2: After filtration, the soil moves into the temporary storage where it is released in a controlled manner to the cuvette and test tube. Once the soil is added to the cuvette and test tube, conveyor 1 reverses its direction.

Step 3: The gantry picks up the test tube and places it on conveyor 2. It picks up the cuvette and places it on conveyor 3. Conveyor 2 moves the test tube to APSX and this test will take some time to complete. Conveyor 3 then moves the cuvette through the sealing mechanism and back.

Step 4: The gantry picks up the cuvette (with lid) from conveyor 3 and brings it to Raman where the test is done. After this is complete the gantry picks up the cuvette and puts it in the storage area.

Step 5: While all this is done, the APSX test will finish. So conveyor 2 will retract now. The gantry will pick up this test tube and put it on conveyor 3 so that it gets sealed. Once this is done the sealed test tube will be transported to the storage area using the gantry.

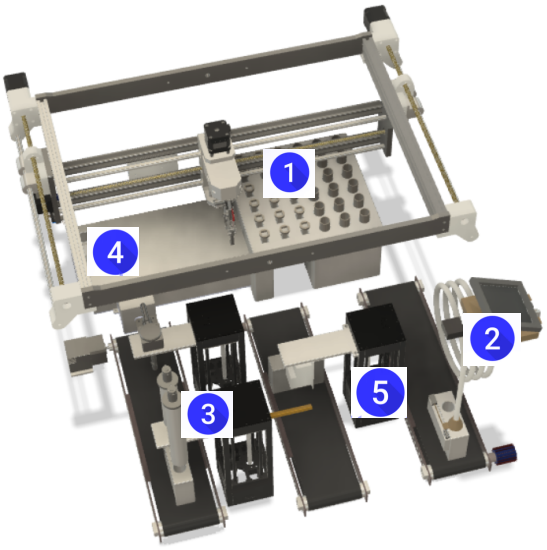

Internal science module.

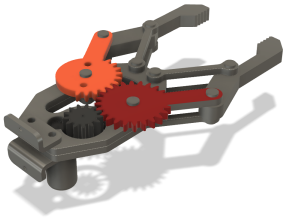

End effector of the gantry.

Cuvette with lid and without lid.

Test tube with lid and without lid.

Pressurised module for ATP testing:

Sequence of steps:

Step 1: The swab dispenser releases the swab for the robotic arm to take the sample.

Step 2: After taking the sample the robotic arm places it in the airlock

Step 3: The swab is cooled and transferred into the testing area where a reagent dispenser readies the enzymes for the test

Step 4: The luminometer detects bioluminescence if present.

Sensors used in Exploration and Mapping

The software mission is divided into three main tasks of complete mapping, autonomous navigation, and imaging in the lava tube. For achieving this autonomous navigation and mapping capability, the rover is equipped with a 360x360 Field of View LiDaR for perception and extraction of Point cloud data. Other than this, we will use a custom Pan-camera for taking high quality images and videos of the lava tube. We will rely on odometry readings for getting the rover coordinates, hence we will rely on wheel odometry, hover map LIDAR's odometry and the tracking cam's visual odometry for getting a precise location.

The LiDAR is similar to a hovermap LiDaR manufactured by Emesent. It has a range of 200 m and can generate 300,000 points per second with a maximum error of 30mm for far away objects. The LiDAR uses e-GaN FET laser drivers, which allows for faster LiDARs with lower inductance packaging, enhanced electrical efficiency, higher currents, and hence improved long-range capabilities [2.8]. The Intel realsense Tracking camera is chosen because it can work even in illumination of 15 lux which will be provided by a constant LED source. The optical sensor will be used for detecting an opening in the lava tube if the mission is done during the day by checking if the illumination of the cave is above a certain threshold.

The Pan-Camera will be equipped with motors that provide 150° of pitch from zenith angle and 180° of yaw, to capture images of the ceiling, ground, walls and any geological formations in the bot’s vicinity. The inlet will have a 30° field of view. The light passes through the first set of lenses, then is reflected at 90° by a mirror, after which it passes through the focusing and zoom lenses. Next, it is adjusted for aperture and passes through one of the spectral narrow-band filters or the movable RGBG quad-Bayer colour filter before incidence on a 12MP radiation-hardened CMOS with 14-bits per channel. The lenses enable up to 50x zoom, and LiDAR depth data guide the focusing adjustment. A xenon flash lamp (strobe light) will use up to 600Ws per flash to illuminate far objects. A 20W LED lamp will be used as a light source for videography and near-object imaging. The pan-cam motors and image sensor will be equipped with image stabilisation to counteract the motion and vibration of the rover.

The images and video will be processed using Deep-Learning techniques to enhance the visual quality of low light images. Using Markov Random Fields, fusing 3D LiDAR data with 2D colour images would also be possible to obtain 3D reconstructions of the environment and geological formations. Further, using Deep Learning, it would be possible to identify and classify the objects in the image, such as rocks and minerals, based on visual qualities. The image and video data will be stored onboard in RAW form. The post-processing will be done at the base station to conserve onboard computing resources and deliver unprocessed data to the scientists for documentations and future research. The camera and lighting will be calibrated on Earth for different conditions to account for varying ambient lighting, speed of the rover, distance to the objects and the terrain. The camera software will be capable of fine-tuning ISO, shutter speed, aperture, zoom and focus adjustment, flash-lighting, camera resolution and lens distortion. Further, the astronauts will be expected to calibrate the camera using fiducial markers and the strobe light timing to ensure the integrity of the camera system before deployment for the mission.

MISSION EXECUTION

The most crucial objective of our mission is to improve the human knowledge of martian lava tubes. Accordingly, the Science rover will be well equipped to conduct various scientific experiments at multiple sites. The scout bots will autonomously explore the lava tube and identify specific places to conduct investigations. These sites which are suitable for further experimentation are called *Regions of Interest (RoI)*. We have classified the following as RoI(s):

1. High Magnetic Field And High Temp region.
2. Unusual Geographic Regions, Mining regions And Trenches.
3. Openings (Skylights and Collapses).
4. Life detection, Habitable regions and Water regions
   (For more details read Software Appendix C1)

Exploration, identification and classification of the RoIs will start as soon as the rover is lowered in the skylight entrance. The science bot and all the four scouts will be programmed to deploy from the skylight base, in different directions. The readings will gather the relevant information to start the exploration in the high-speed data transmission region, such as the cave's width, directions of openings, and the geological features that will determine the navigation algorithm and speed of the robots. At the start of the mission, the scout bots detach from the Science rover and begin their exploration and mapping. For the entire journey, the scout bots will use a wall following method. This is because the lava tubes' width can be as large as 400m, the rover can lose track of features and get lost in the tube. Based on the LIDAR data [4.4], all scout bots will determine the frontiers present in the lava tube and the base station will assign frontiers to each rover to avoid multiple rovers exploring along the same wall. After this, all rovers will follow a wall using the frontier assignment and continue moving deep into the cave.

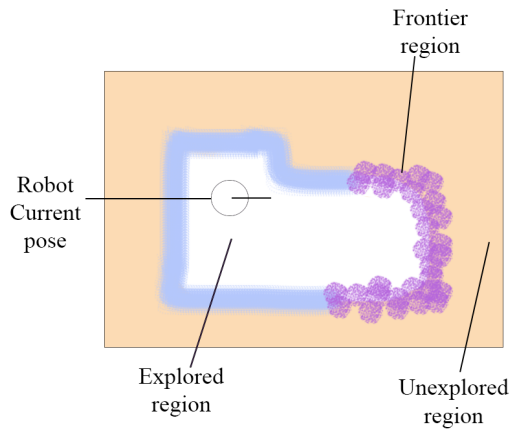

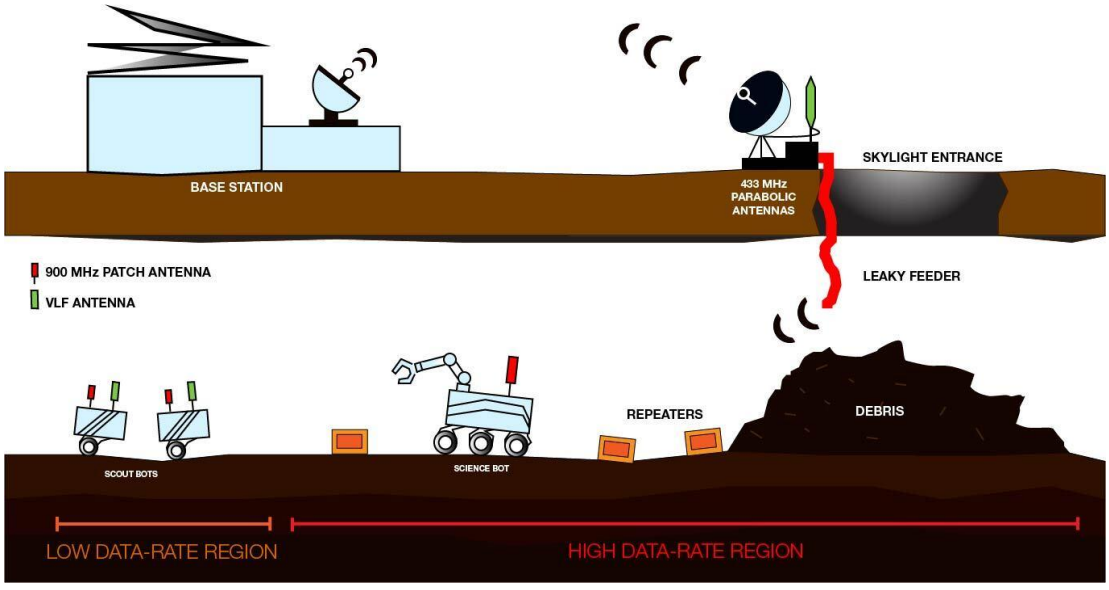

We plan on using two rovers for parallel exploration as it increases the efficiency of the process, and due to mobility constraints, the rovers need to tether together to overcome difficult terrains and obstacles. Figure Schematic of Data Resions

Simultaneous Localization and Mapping (SLAM) is done with bots being in a mesh network and communicating their point cloud data with each other using the high speed 44Mbps-73 Mbps link provided by patch antennas. A multi-robot SLAM procedure is proposed because multiple robots explore around the same region and thus having multiple robots working on the same map will guarantee a smaller error in pose estimation of the individual robots as well as help in minimizing the bundle adjustment error. Each scout will gather points cloud data from their own LiDARs. The SLAM process will be done keeping in mind the priority order of the scouts. All scouts will transmit their LiDaR readings to the highest priority scout, which will do the SLAM backend [4.11] and share the merged data to all bots currently in the mesh network to increase compute efficiency and reduce compute latency in all the bots. Map update will be done based on the linear distance travelled OR angular distance covered, and the bot in mesh, which reaches the threshold first, will signal the highest priority bot to stitch the latest point cloud readings and make a global map. To accommodate point-cloud in the transmission limit, we first convert the point cloud data from LAS format to standard compression LAZ format and then ZIP compress it. This reduces the point cloud data by a factor of 14. This compressed cloud is then transmitted to the base station, and the updated transformation and optimization matrix of point cloud data of each scout bot is transmitted back to all the scouts currently in the mesh network so that each of them can update their map given their current LiDaR readings.

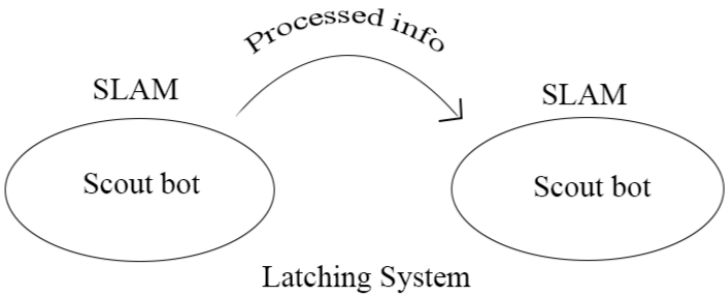

Imaging and Videography of the environment would be done with the high resolution camera of the PanCam. Due to the low-lighting conditions of the lava tubes, artificial lighting will be imperative for proper imaging of the scene. Images will be taken both with and without light. After deployment of the scout bots, the onboard computer will adjust the camera and lighting settings to suit the scout's speed, the ambient lighting, and the surrounding environment. The frequency of image capture will vary depending on the availability of power for the flashlight, the speed of the scout bot and the time needed to adjust the camera. It is expected to be one image every 5 to 10 seconds. However, should the bot recognise a region of special interest, it may increase this frequency to capture more detail of the environment. The scout bot may stop at a certain point to further investigate the region and collect, in addition to colour images, video of the surroundings, images using spectral filters and thermal emission spectrographs of the field of view for further analysis [4.1].

High Data Region would include the scout bots having two additional tasks other than exploration: dropping repeaters to establish a region with a high-speed data link and identifying

regions of interest and sending this data to the base station. For establishing the high-speed data link, a repeater node is dropped from a bot if the Received Signal Strength Indicator (RSSI) between the bot and its nearest dropped node is below a set threshold. RSSI is an estimated measure of the power level that an RF client device is receiving from an access point or router. As the distance between radio transceivers increases the value of RSSI decreases which leads to slower data rates. The scout bots will try to drop the repeaters in the centre of the cave so that the range is maximized. For identifying ROIs, the scout bots track all the atmospheric conditions' sensors onboard it and compare the reading to a pre-set threshold. If 2 or more factors are in the favourable ranges, it stops to conduct a miniTES and Digital Holographic Imaging test. It sends all the data of the live atmospheric conditions' tests as well as the data from the miniTES and Digital Holographic Imaging to the base station.

After 3 kilometres have been traversed by the scout bot, an algorithm at the base station will choose the 15 best sites for further scientific testing. These sites will be present at the same side of the tunnel due to the mobility constraints of the science rover. As the science bot stays in the High Data Rate region, it will be possible for us to Manually Operate the science rover at all times. In case of communication failure, the Science rover will have enough *autonomous capability* to track its traversed path and return to the skylight entrance, and when reestablished, it can shift back to manual operation. In the Science bot, the high-resolution camera mounted at the top of the mast will provide color and multispectral images of the site, followed by Mini-TES providing remotely-sensed point discrimination of mineral composition of the terrain features. The texture, granularity, and other surface features of the points with high mineral content will be analyzed using the microscope mounted on the arm. The surface will also be analyzed for possible biofilms and microbial mats using the ATP Bioluminescence test. Ground-penetrating radar will provide information on the presence of the region's subsurface water, ice, and stratigraphic profile. This data will be stored in the onboard computer and will be processed in the base station to understand geological history, spatial heterogeneity, and the potential of origin and survival of life beneath the sub-surface. The site will then be drilled for the sampling of interior unoxidized surface or rock samples. The dust formed due to drilling will be collected using the soil collection mechanism name and transported to the Raman spectrometer cuvette, where it will be analyzed for potential biosignatures such as amino acids, lipids, sterols, hopanoids, and carbohydrates. It will be succeeded by elemental analysis through an Alpha Particle X-ray spectrometer. The drilled opening will also undergo an ATP bioluminescence test to detect traces of ATP. If co-occurring concentrations of biologically important molecules and minerals are detected or microscopic, and GPR analysis reveals heterogeneity suggestive of biological morphologies, the sample will be stored in the buffer box for further analysis at the base station. During manual operation, a live feed of a camera mounted on the science rover will be sent to the operator who will, in return, the corresponding telemetry data. Science testing at the 15 selected sites and the all, the live science data will be sent to the base station for further autonomous or manual analysis.

In order to maximize the chances of detecting biosignatures using the science rover, we aim to find sites with high exobiology potential. We will be looking for the sites that date back to Mars' early, life-friendly period, i.e., the Noachian to the Noachian/Hesperian boundary, or sites with subsurface ice, aqueous sediments, or minerals that can preserve organic biomarkers. Such sites can also contain minerals indicating past favorable conditions for liquid water or standing water,

thermal spring environments, and the aqueous weathering processes. Sites containing minerals with high preservation potential for biosignatures, or minerals derived from elements essential for sustenance of life like sodium, magnesium, calcium also form the region of interest. Minerals such as olivine that are known to contain life in Mars analogous earth environments are also classified as potential sites for scientific analysis.

After minerals favorable to life are detected at a particular site, biological analysis is conducted. A promising biomarker for life detection can be defined as a chemical species or topographical pattern uniquely derived from living organisms and must not be synthesized abiotically, thus unambiguously indicating the presence of extinct or extant life. The biomarkers being detected by the science module have been put into three broad categories based on a priority order. The first priority consists of biomarkers belonging to a strictly biogenic origin, which are conclusive of extant and extinct lifeforms. The next priority level includes organic compounds, which come from both biotic and abiotic sources. It also includes minerals that are often produced as a result of biologically induced processes. The last priority level contains the biomarkers and minerals that do not have any biotic source yet can help understand the Martian conditions in detail. Refer to Appendix D.1. Based on the biomarkers and minerals detected at various priority levels by the science module, it can be determined how good the site is as a region of interest.

When the scout bot crosses the 3 km mark and enters the low bandwidth region, it will cease the live stream of data from atmospheric sensors to the base station. The data will be stored on the rover, and any location where the atmospheric parameters cross a threshold value will be marked.

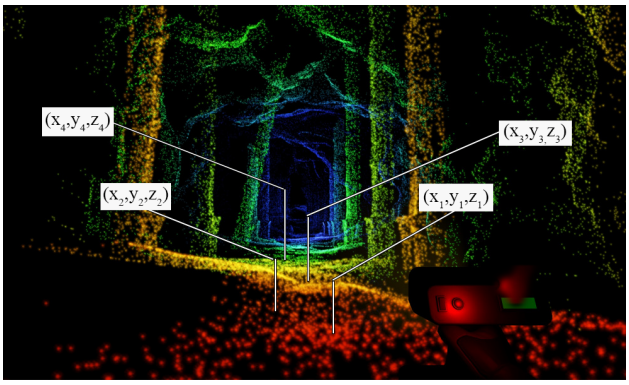

As in the figure on the left. Coordinates will be flagged while moving inside the cave, the rover will mark various nodes on the map as waypoints. This *Graph-node* will record the coordinates and the orientation of the rover. A new Graph-node will be created regularly every second. Also, a *Region of Interest graph-node* will be recorded as soon as a RoI is identified and all the current coordinates and atmospheric sensors' data will be recorded. The low data rate region has a consistent data transfer link of 50 Bytes, per second, we will only send the essential data to the base station. This means we will use the link to send encoded robot status to the base station every 5 seconds(refer to Appendix 3.3.4). Other than this, the scout bot will also send its current Graph-node to the base station once every 30 seconds and an encoded RoI node will be transmitted to the base station whenever a RoI node is created.

This is also the region in which the scout bot can encounter forks and big obstacles. In case the scout bots exploring one side of the lava tube encounter a fork and the rovers detect that their line of sight communication is obstructed, and in the map they generate, there exists a wall-like obstacle in between them, it can be classified as a junction. When the rover identifies a junction,

they will follow their specific walls and explore the different branches of the cave. They will continue this exploration for 100m and record atmospheric data, slope, and gradients of these factors. If the line of sight communication is re-established between these rovers, the junction will be considered a significant obstacle; otherwise, The scout bot will compare the "exploration potential" of both branches, a weighted sum of all these recorded factors. After this, the scout bots will start moving back to the branches' junction until the line of sight is reestablished and explore the *more promising* branch. The rover that recorded a better exploration potential will stay put at the junction, while the other will start moving towards the first rover until it detects a wall on one side. The second rover will now consider this new wall to follow, and the two rovers will start exploring the new branch together. The scout bots will also keep track of the exploration potential and keep adding weighted factors like gradient changes in atmospheric factors, slope and the distance from the junction. This is what we may call *The cost of returning*. If the returning costs become negative, the rovers will start moving back to the intersection and choosing the other branch instead. If the rovers detect an obstacle covering the cave's width, they will try to go over the block. Using point cloud data, we will check if the obstruction is traversable and act accordingly. Forgoing over the obstacle, it needs to tether with the other scout bot and start climbing. If a collapse or an untraversable obstacle is detected, the rover will begin to return to the base skylight. While moving deep inside the lava tubes, the scout bots keep looking for regions of interest. It records all the sensor readings at all points, and if the various data it gets are favourable, they flag these affiliated sites on the map it builds. All these sites are regions of interest, and the rover would use the data it collected to create a list of places it needs to stop for further tests and soil collection after its onside trip has completed.

Returning Mechanism is based on various factors like remaining battery, distance from the base skylight, time to get back, time to be taken for stopping at 40 sites to conduct tests and collect samples, a *Returning Algorithm* will decide when the rover should turn back. The Graph-nodes that the rover had created can be used as waypoints the rover can use for returning to the base station. From all the RoIs that the scout bot encountered while exploring the cave, it will then choose the top 40 regions of interest and, while returning, stop to conduct miniTES and digital holographic imaging tests and collect soil samples of these sites, to help scientists in researching more geographic and biological data of the martian lava tube. After the rover reaches the base skylight, its data-storage can be extracted to retrieve and visualise all the collected map, imaging, video and science data it has collected in the 10 hours of the mission.

CONCLUSION

The plan proposed in this report aims to execute a comprehensive survey of the Martian Lava tubes in 10 hrs. The four scout bots traverse, navigate and investigate the rough terrain, collecting a wealth of information in the form of images, videos and preliminary scientific measurements. The science bot further investigates specific regions of interest and performs a more comprehensive analysis of the environment and collects scientific data and samples. All the bots perform their tasks while maintaining a constant communication link with the astronauts allowing them to monitor the mission and make crucial decisions. This mission will allow humans to better understand the red planet and explore the possibility of habitation on Mars.

FUTURE SCOPE

Though our proposed mission aims at exploring the lava tubes for a duration of 10 hours, this mission unlocks the possibility and scope of research many-fold. The proposed mission and rovers themselves can be used for missions conducted at various different skylight entrances that are discovered. The mission will reveal a lot more information about the scientific details of the martian lava tubes, which may open new possibilities for martian habitability and exploration.

Citation & References:

1. Mechanical

1. https://www.ati-ia.com/products/toolchanger/ManualToolChanger.aspx?s=1
2. https://onrobot.com/sites/default/files/documents/Datasheet_QuickChangers_v1.2_EN.pdf
3. Anttila, M., 2005. *Concept evaluation of Mars drilling and sampling instrument*. Espoo: Helsinki University of Technology.
4. https://www.esmats.eu/amspapers/pastpapers/pdfs/2012/phillips.pdf
5. https://onrobot.com/sites/default/files/documents/Datasheet_QuickChangers_v1.2_EN.pdf
6. https://www.maxongroup.com/maxon/view/content/index
7. Nesnas, I.A., Matthews, J.B., Abad-Manterola, P., Burdick, J.W., Edlund, J.A., Morrison, J.C., Peters, R.D., Tanner, M.M., Miyake, R.N., Solish, B.S. and Anderson, R.C. (2012), Axel and DuAxel rovers for the sustainable exploration of extreme terrains. J. Field Robotics, 29: 663-685, https://doi.org/10.1002/rob.21407
8. Francesco Sauro, Riccardo Pozzobon, Matteo Massironi, Pierluigi De Berardinis, Tommaso Santagata, Jo De Waele, Lava tubes on Earth, Moon and Mars: A review on their size and morphology revealed by comparative planetology, Earth-Science Reviews, Volume 209, 2020, 103288, ISSN 0012-8252, https://doi.org/10.1016/j.earscirev.2020.103288.
9. Firat Barlas (2014). Design of Mars Rover Suspension Mechanism (Dissertation). Retrieved from https://core.ac.uk/display/324141778?recSetID=
10. Lawton, N. (2020). Planetary Rover Wheel and Lower Leg Structural Design to Reduce Rock Entanglements (Dissertation). Retrieved from http://urn.kb.se/resolve?urn=urn:nbn:se:ltu:diva-78565
11. Matthew J. Roman and Norman, Oklahoma (2005). Design and Analysis of a Four Wheeled Planetary Rover (Thesis). Retrieved from http://c3p0.ou.edu/IRL/Theses/Roman-MS.pdf
12. Lan, T.T. (1998). Space Frame Structures.
13. *Advantages of Aluminium Honeycomb Panels Compared To Traditional Building Materials:* (2018, January 30). Gilcrest Manufacturing. https://www.gilcrestmanufacturing.com/news/technical-news/advantages-aluminium-honeycomb-panels-compared-traditional-building-materials/

2. Electrical

1. *No.97CH6203)*, 1997, pp. 749-752 vol.1, doi: 10.1109/IECEC.1997.659285.

2. NASATribo : Dunbar, B. (2005, October 8). *Crackling planets*. NASA. https://www.nasa.gov/vision/space/livinginspace/10aug_crackling.html.

3. Rahman, Md & Rashid, Sm Hasanur & Hassan, Km Rafidh & Hossain, Muhammad. (2018). Comparison of Different Control Theories on a Two Wheeled Self Balancing Robot. AIP Conference Proceedings. 1980. 060005. 10.1063/1.5044373.

4. Antunes, S. (2012). (rep.). DIY satellite platforms: Building a space-ready general base picosatellite for any mission. Retrieved from http://marspedia.org/Outgassing#cite_note-Antunes1-3

5. S. Murugesan, "An Overview of Electric Motors for Space Applications," in IEEE Transactions on Industrial Electronics and Control Instrumentation, vol. IECI-28, no. 4, pp. 260-265, Nov. 1981, doi: 10.1109/TIECI.1981.351050.

6. Phillips, R. (n.d.). *5 challenges an electric motor has to overcome on Mars*. drive.tech. https://drive.tech/en/stream-content/5-challenges-an-electric-motor-has-to-overcome-on-mars.

7. Kemp, M. A., Franzi, M., Haase, A., Jongewaard, E., Whittaker, M. T., Kirkpatrick, M., & Sparr, R. (2019, April 12). *A high Q PIEZOELECTRIC resonator as a portable VLF transmitter*. Nature News. https://www.nature.com/articles/s41467-019-09680-2.

8. Wikimedia Foundation. (2021, June 12). *Leaky feeder*. Wikipedia. https://en.wikipedia.org/wiki/Leaky_feeder.

9. Ahmadi, S. (n.d.). *Orthogonal frequency division multiple access*. Orthogonal Frequency Division Multiple Access - an overview | ScienceDirect Topics. https://www.sciencedirect.com/topics/engineering/orthogonal-frequency-division-multiple-access.

10. J. Shibalabala and T. G. Swart, "Performance Analysis of Wireless Mesh Networks for Underground Mines," *2020 International Conference on Artificial Intelligence, Big Data, Computing and Data Communication Systems (icABCD)*, 2020, pp. 1-6, doi: 10.1109/icABCD49160.2020.9183849.

11. W. Walsh and J. Gao, "Communications in a cave environment," *2018 IEEE Aerospace Conference*, 2018, pp. 1-8, doi: 10.1109/AERO.2018.8396606.

12. Petach, M., & Tward, M. (2018). (tech.). *Thermoacoustic Power Convertor (TAPC)* (pp. 1–68). NASA.

13. NASA. (n.d.). (tech.). *Multi-Mission Radioisotope Thermoelectric Generator (MMRTG)* (pp. 1–2).

14. Withrow, J. P. (2012). (tech.). *ADVANCED STIRLING RADIOISOTOPE GENERATOR FLIGHT DEVELOPMENT* (pp. 1–2). Nuclear and Emerging Technologies for Space.

15. Lewandowski, Edward & Oriti, Salvatore & Schifer, Nicholas. (2015). Characterization of the Advanced Stirling Radioisotope Generator EU2. 10.2514/6.2015-3808.

16. Sion Power. (2021). *Modular Power Pack*. Tuscon, Arizona; Sion Power - Modular Power Packs.

17. XP Power. (2020). *ASB110 Series*. XP Power - ASB110 Series.

18. Aurbach, Doron & Chusid, O.. (2009). SECONDARY BATTERIES – LITHIUM RECHARGEABLE SYSTEMS | Electrolytes: Additives. 10.1016/B978-044452745-5.00208-2.
Wang, Renheng & Cui, Weisheng & Chu, Fulu & Wu, Feixiang. (2020). Lithium metal anodes: Present and future. Journal of Energy Chemistry. 48. 10.1016/j.jechem.2019.12.024.

19. Lang, Jialiang & Qi, Longhao & Luo, Yuzi & Wu, Hui. (2017). High Performance Lithium Metal Anode: Progress and Prospects. Energy Storage Materials. 7. 10.1016/j.ensm.2017.01.006.

20. Luo, Zheng & Qiu, Xuejing & Liu, Cheng & Li, Shuo & Wang, Chiwei & Zou, Guoqiang & Hou, Hongshuai & Ji, Xiaobo. (2021). Interfacial challenges towards stable Li metal anode. Nano Energy. 79. 105507. 10.1016/j.nanoen.2020.105507.

3. Science

1. Bates, D., Silverman, S., Jeter, J., Blasius, K., Christensen, P., & Mehall, G. (2000). Performance of the miniature thermal emission spectrometer (Mini-TES) for Mars 2001 Lander. *2000 IEEE Aerospace Conference. Proceedings (Cat. No.00TH8484)*, *3*, 135–149 vol.3. https://doi.org/10.1109/AERO.2000.879842

2. Christensen, P. R., Ruff, S. W., Fergason, R. L., Knudson, A. T., Anwar, S., Arvidson, R. E., Bandfield, J. L., Blaney, D. L., Budney, C., Calvin, W. M., Glotch, T. D., Golombek, M. P., Gorelick, N., Graff, T. G., Hamilton, V. E., Hayes, A., Johnson, J. R., McSween Jr., H. Y., Mehall, G. L., … Wyatt, M. B. (2004). Initial results from the Mini-TES experiment in Gusev crater from the Spirit rover. In *Science* (Vol. 305, Issue 5685, p. 6). https://doi.org/10.1126/science.1100564

3. Ciarletti, V., Clifford, S., Plettemeier, D., Le Gall, A., Hervé, Y., Dorizon, S., Quantin-Nataf, C., Benedix, W.-S., Schwenzer, S., Pettinelli, E., Heggy, E., Herique, A., Berthelier, J.-J., Kofman, W., Vago, J. L., & Hamran, S.-E. (2017). The WISDOM Radar: Unveiling the Subsurface Beneath the ExoMars Rover and Identifying the Best Locations for Drilling. *Astrobiology*, *17*(6–7), 565–584. https://doi.org/10.1089/ast.2016.1532
4. Coates, A. j., Jaumann, R., Griffiths, A. d., Leff, C. e., Schmitz, N., Josset, J.-L., Paar, G., Gunn, M., Hauber, E., Cousins, C. r., Cross, R. e., Grindrod, P., Bridges, J. c., Balme,

M., Gupta, S., Crawford, I. a., Irwin, P., Stabbins, R., Tirsch, D., … the, P. T. (2017). The PanCam Instrument for the ExoMars Rover. *Astrobiology*, *17*(6–7), 511–541. https://doi.org/10.1089/ast.2016.1548

5. De Angelis, A., Managò, S., Ferrara, M. A., Napolitano, M., Coppola, G., & De Luca, A. C. (2017). Combined Raman Spectroscopy and Digital Holographic Microscopy for Sperm Cell Quality Analysis. *Journal of Spectroscopy*, *2017*, e9876063. https://doi.org/10.1155/2017/9876063

6. Desta, F., & Buxton, M. (2017). *The use of RGB Imaging and FTIR Sensors for Mineral mapping in the Reiche Zeche underground test mine, Freiberg*.

7. Ditto, T. (2018). *HOMES: Holographic Method for Exoplanet Spectroscopy*. https://ntrs.nasa.gov/citations/20190001161

8. Fornaro, T., Steele, A., & Brucato, J. R. (2018). Catalytic/Protective Properties of Martian Minerals and Implications for Possible Origin of Life on Mars. *Life (Basel, Switzerland)*, *8*(4), E56. https://doi.org/10.3390/life8040056

9. Herkenhoff, K. E., Squyres, S. W., Bell, J. F., Maki, J. N., Arneson, H. M., Bertelsen, P., Brown, D. I., Collins, S. A., Dingizian, A., Elliott, S. T., Goetz, W., Hagerott, E. C., Hayes, A. G., Johnson, M. J., Kirk, R. L., McLennan, S., Morris, R. V., Scherr, L. M., Schwochert, M. A., … Wadsworth, M. V. (2003). Athena Microscopic Imager investigation. *Journal of Geophysical Research: Planets*, *108*(E12). https://doi.org/10.1029/2003JE002076

10. *Holographic Sensors: Three-Dimensional Analyte-Sensitive Nanostructures and Their Applications | Chemical Reviews*. (n.d.). Retrieved August 15, 2021, from https://pubs.acs.org/doi/10.1021/cr500116

11. Horgan, B. H. N., Cloutis, E. A., Mann, P., & Bell, J. F. (2014). Near-infrared spectra of ferrous mineral mixtures and methods for their identification in planetary surface spectra. *Icarus*, *234*, 132–154. https://doi.org/10.1016/j.icarus.2014.02.031

12. Life, N. R. C. (US) C. on the O. and E. of. (2002). Detecting Extant Life. In *Signs of Life: A Report Based on the April 2000 Workshop on Life Detection Techniques*. National Academies Press (US). https://www.ncbi.nlm.nih.gov/books/NBK223875/

13. Liu, Z., Rossi, J.-C., & Pascal, R. (2019). How Prebiotic Chemistry and Early Life Chose Phosphate. *Life*, *9*(1), 26. https://doi.org/10.3390/life9010026

14. Marshall, C. P., & Marshall, A. O. (2014). Raman spectroscopy as a screening tool for ancient life detection on Mars. *Philosophical Transactions of the Royal Society A: Mathematical, Physical and Engineering Sciences*, *372*(2030), 20140195. https://doi.org/10.1098/rsta.2014.0195

15. Milshteyn, D., Blank, J., & Moser, D. (2019). *ATP Bioluminescence Assay as a Proxy for Life Detection Methods in Subsurface Analog Sites*.

16. Neveu, M., Hays, L. E., Voytek, M. A., New, M. H., & Schulte, M. D. (2018). The Ladder of Life Detection. *Astrobiology*, *18*(11), 1375–1402. https://doi.org/10.1089/ast.2017.1773

17. Popa, R., Smith, A. R., Popa, R., Boone, J., & Fisk, M. (2012). Olivine-Respiring Bacteria Isolated from the Rock-Ice Interface in a Lava-Tube Cave, a Mars Analog Environment. *Astrobiology*, *12*(1), 9–18. https://doi.org/10.1089/ast.2011.0639

18. Shanmugam, M., Vadawale, S. V., Patel, A. R., Mithun, N. P. S., Adalaja, H. K., Ladiya, T., Goyal, S. K., Tiwari, N. K., Singh, N., Kumar, S., Painkra, D. K., Hait, A. K., Patinge, A., Kumar, A., Basha, S., Subramanian, V. R., Venkatesh, R. G., Prashant, D. B., Navle, S., … Bhardwaj, A. (2019). Alpha Particle X-Ray Spectrometer (APXS) On-board Chandrayaan-2 Rover—Pragyan. *ArXiv:1910.09232 [Astro-Ph, Physics:Physics]*. http://arxiv.org/abs/1910.09232

19. WISDOM (radar). (2021). In *Wikipedia*. https://en.wikipedia.org/w/index.php?title=WISDOM_(radar)&oldid=1026940362

20. Yetisen, A. K., Naydenova, I., da Cruz Vasconcellos, F., Blyth, J., & Lowe, C. R. (2014). Holographic sensors: Three-dimensional analyte-sensitive nanostructures and their applications. *Chemical Reviews*, *114*(20), 10654–10696. https://doi.org/10.1021/cr500116

21. Cavalazzi, B., & Westall, F. (Eds.). (2019). *Biosignatures for Astrobiology*. Springer International Publishing. https://doi.org/10.1007/978-3-319-96175-0

22. Czamara, K., Majzner, K., Pacia, M. Z., Kochan, K., Kaczor, A., & Baranska, M. (2015). Raman spectroscopy of lipids: A review. *Journal of Raman Spectroscopy*, *46*(1), 4–20. https://doi.org/10.1002/jrs.4607

23. Edwards, H. G. M., Hutchinson, I. B., Ingley, R., & Jehlička, J. (2014). Biomarkers and their Raman spectroscopic signatures: A spectral challenge for analytical astrobiology. *Philosophical Transactions of the Royal Society A: Mathematical, Physical and Engineering Sciences*, *372*(2030), 20140193. https://doi.org/10.1098/rsta.2014.0193

24. Griffith, W. P. (1969). Raman Spectroscopy of Minerals. *Nature*, *224*(5216), 264–266. https://doi.org/10.1038/224264a0

25. Hutchinson, I. B., Ingley, R., Edwards, H. G. M., Harris, L., McHugh, M., Malherbe, C., & Parnell, J. (2014). Raman spectroscopy on Mars: Identification of geological and bio-geological signatures in Martian analogues using miniaturized Raman spectrometers. *Philosophical Transactions of the Royal Society A: Mathematical, Physical and Engineering Sciences*, *372*(2030), 20140204. https://doi.org/10.1098/rsta.2014.0204

26. Jorge Villar, S. E., & Edwards, H. G. M. (2006). Raman spectroscopy in astrobiology. *Analytical and Bioanalytical Chemistry*, *384*(1), 100–113. https://doi.org/10.1007/s00216-005-0029-2

27. H. G. M. Edwards, I. B. Hutchinson, R. Ingley, and J. Jehlička, "Biomarkers and their Raman spectroscopic signatures: a spectral challenge for analytical astrobiology," *Philosophical Transactions of the Royal Society A: Mathematical, Physical and Engineering Sciences*, vol. 372, no. 2030, p. 20140193, Dec. 2014, doi: 10.1098/rsta.2014.0193

28. BOSTON, P. J., SPILDE, M. N., NORTHUP, D. E., MELIM, L. A., SOROKA, D. S., KLEINA, L. G., LAVOIE, K. H., HOSE, L. D., MALLORY, L. M., DAHM, C. N., CROSSEY, L. J., & SCHELBLE, R. T. (2001). Cave Biosignature Suites: Microbes, Minerals, and Mars. *ASTROBIOLOGY Volume 1, Number 1, 2001 Mary Ann Liebert, Inc.*, *1*. https://doi.org/10.1089/153110701750137413

29. Csuka, J. M., Adeli, S., Baqué, M., Iakubivskyi, I., Kopacz, N., Neubeck, A., Schnürer, A., Singh, A., Stockwell, B. R., Vilhelmsson, O., & Geppert, W. D. (2020). LINKING BIOLOGICAL AND GEOCHEMICAL DATA FROM ICELANDIC LAVA TUBES: INSIGHTS FOR UPCOMING MISSIONS IN THE SEARCH FOR EXTANT OR EXTINCT LIFE ON MARS. *3rd International Planetary Caves Conference, Held 18-21 February, 2020 in San Antonio, Texas. LPI Contribution No. 2197, 2020, Id.1051*.

30. J. Le´veille, R., & Datta, S. (n.d.). Lava tubes and basaltic caves as astrobiological targets on Earth and Mars: A review. *Planetary and Space Science*. https://doi.org/0.1016/j.pss.2009.06.004

31. Paris, A., Davies, E., Tognetti, L., & Zahniser, C. (2020). Prospective Lava Tubes at Hellas Planitia. *ArXiv:2004.13156 [Astro-Ph]*. http://arxiv.org/abs/2004.1315

32. Phillips-Lander, C. M., Agha-Mohammadi, A., Wynne, J. J., Titus, T. N., Chanover, N., Demirel-Floyd, C., Uckert, K., Williams, K., Wyrick, D., Blank, J., Boston, P., Mitchell, K., Kereszturi, A., Martin-Torres, J., Shkolyar, S., Bardebelias, N., Datta, S., Retherford, K., Sam, L., … Weins, R. (2021). Mars Astrobiological Cave and Internal habitability Explorer (MACIE): A New Frontiers Mission Concept. *ArXiv:2105.05281 [Astro-Ph]*. http://arxiv.org/abs/2105.05281

33. Rettberg, P., Rabbow, E., Panitz, C., & Horneck, G. (2004). Biological space experiments for the simulation of Martian conditions: UV radiation and Martian soil analogs. *Advances in Space Research*, *33*(8), 1294–1301. https://doi.org/10.1016/j.asr.2003.09.050

34. Williford, K. H., Farley, K. A., Stack, K. M., Allwood, A. C., Beaty, D., Beegle, L. W., Bhartia, R., Brown, A. J., de la Torre Juarez, M., Hamran, S.-E., Hecht, M. H., Hurowitz, J. A., Rodriguez-Manfredi, J. A., Maurice, S., Milkovich, S., & Wiens, R. C. (2018). Chapter 11—The NASA Mars 2020 Rover Mission and the Search for Extraterrestrial Life. In N. A. Cabrol & E. A. Grin (Eds.), *From Habitability to Life on Mars* (pp. 275–308). Elsevier. https://doi.org/10.1016/B978-0-12-809935-3.00010-4

4. Software

1. O. Aydogan and E. Tasal, “Designing and building a 3D printed low cost modular Raman spectrometer”, *CIJ*, vol. 2, no. 2, pp. 3-14, Dec. 2018.

2. Fast wall-following exploration with two cooperating mobile robots. (n.d.). https://ieeexplore.ieee.org/document/5637013

3. Flash.(n.d.).https://www.electroncomponents.com/20W-LED-high-power-light-emiting-diode

4. Hovermap - LIDAR. (n.d.). https://www.emesent.io/hovermap/

5. Image enhancement techniques. (n.d.). https://www.lkouniv.ac.in/site/writereaddata/siteContent/20200402191015688 3ajay_misra_geo_Digital_Image_Enhancement.pdf

6. Lava tubes on Earth, Moon and Mars: A review on their size and morphology revealed by comparative planetology. (n.d.). https://www.sciencedirect.com/science/article/abs/pii/S0012825220303342

7. Mesh Networking. (n.d.). https://en.wikipedia.org/wiki/Mesh_networking

8. Robotics, S. (n.d.). Simultaneous Localization and Mapping. Wikipedia. SLAM

9. SLAM. (n.d.). https://en.wikipedia.org/wiki/Simultaneous_localization_and_mapping

10. SLAM backend. (n.d.). https://mitpress.mit.edu/books/probabilistic-robotics

11. SVMs. (n.d.). https://en.wikipedia.org/wiki/Support-vector_machine

12. Width of lava tubes: https://www.sciencedirect.com/science/article/abs/pii/S0012825220303342

13. Flat lava tubes: https://www.isas.jaxa.jp/e/forefront/2010/haruyama/

14. Temperature on Mars: https://www.nasa.gov/audience/forstudents/5-8/features/nasa-knows/what-is-mars-58.html

Appendix A: Mechanical

A1. Structure

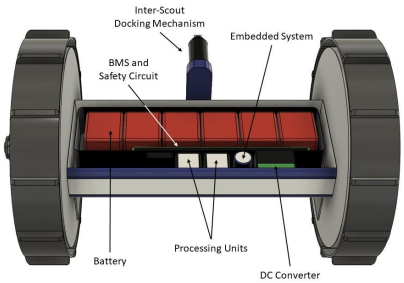

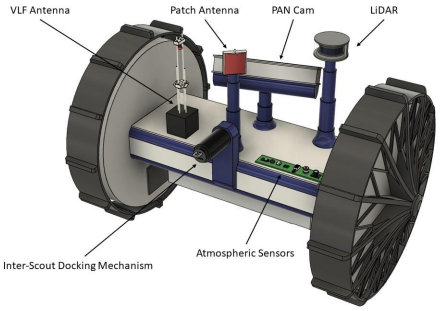

Double Lambda System Mechanism Characteristics

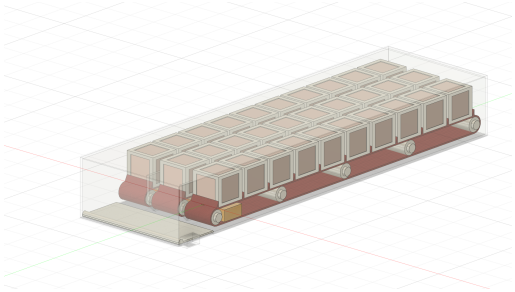

Science Modules on the Scout Bot

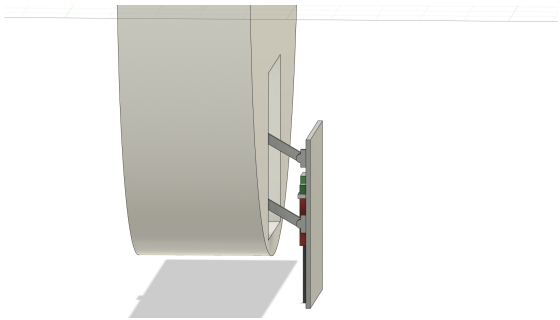

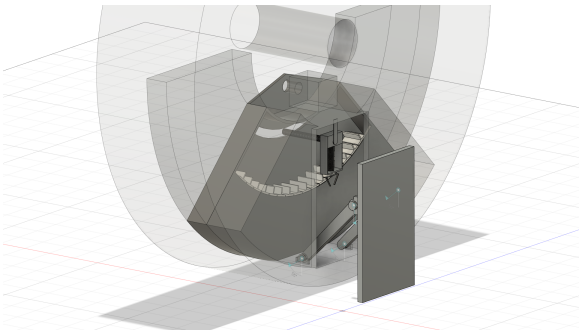

Science Bot Chassis

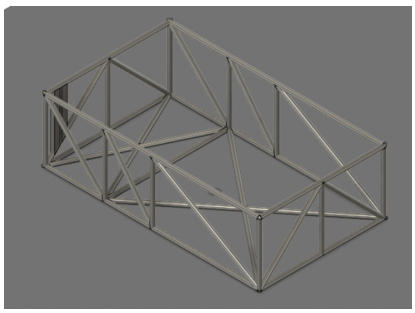

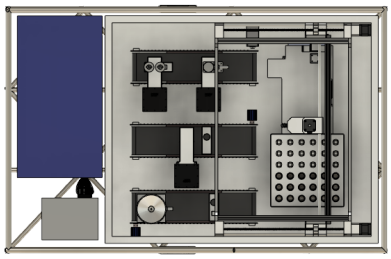

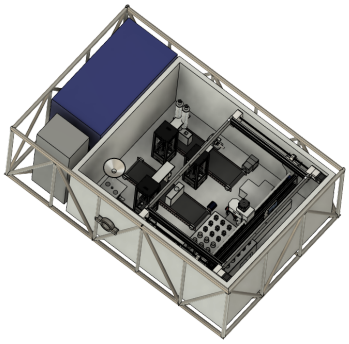

Science Bot Mobility

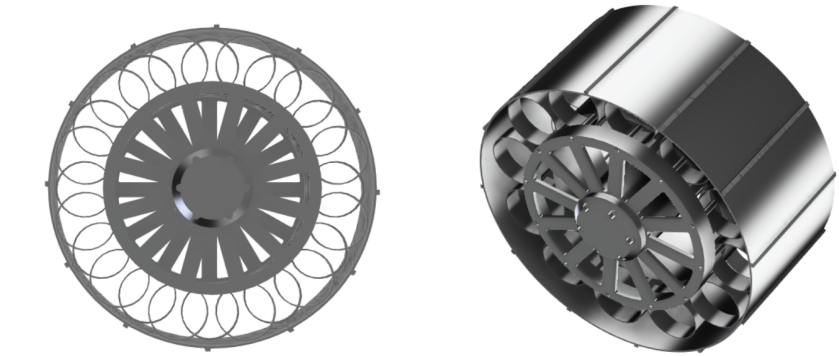

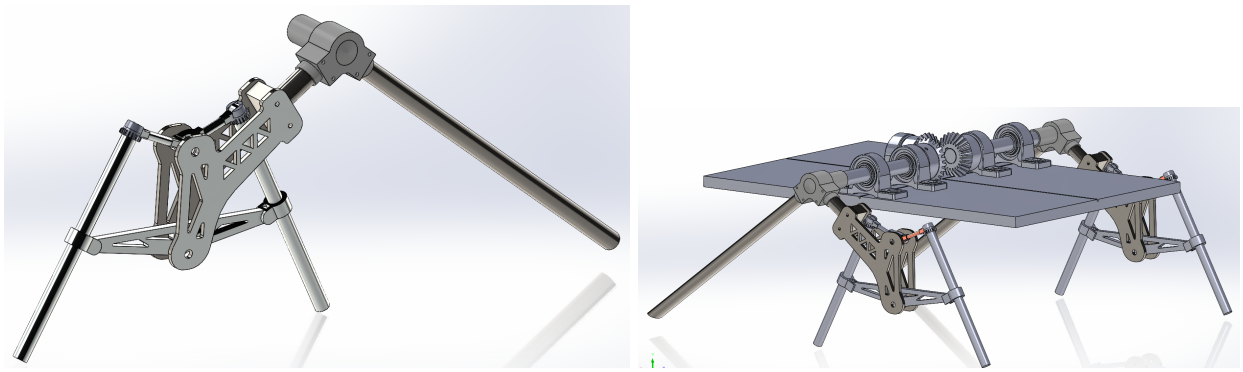

Multiobjective optimization of the wheel was performed considering the following factors:

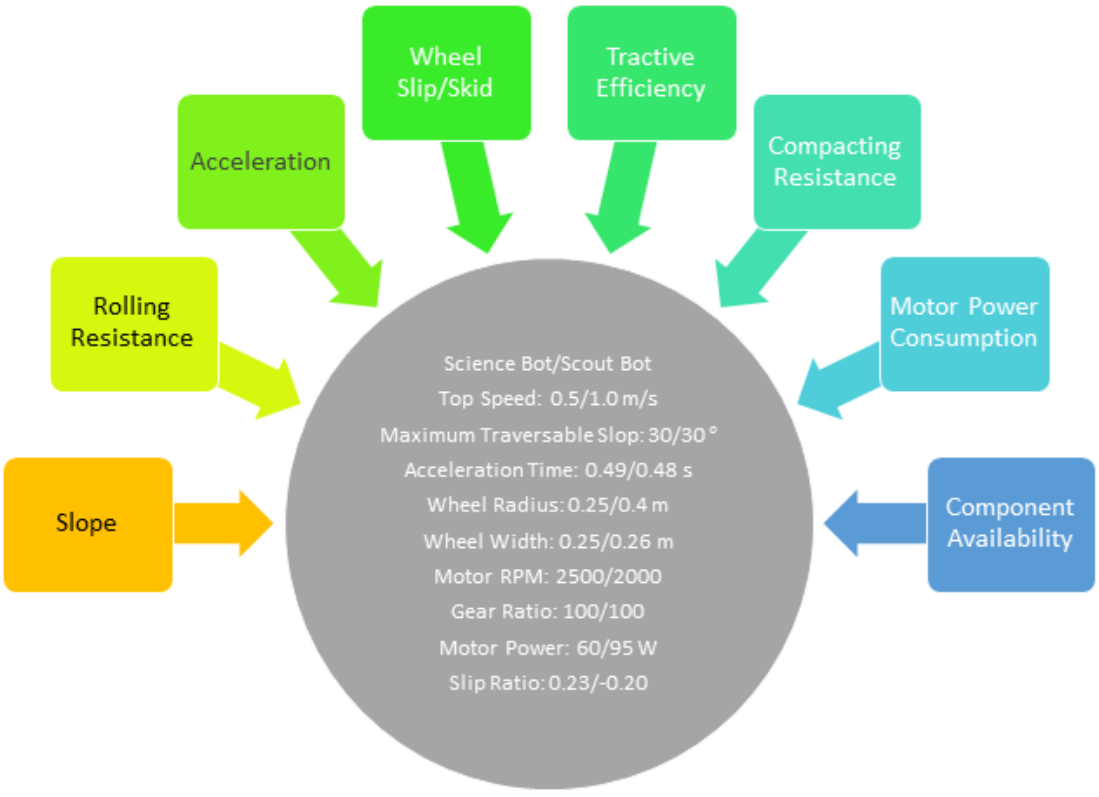

Custom python scripts were used for the optimization of the wheels and are given below.

Science Bot:

```
from gekko import GEKKO
import numpy as np

#Initialize model
m = GEKKO(remote=False)

#define parameter
eq = m.Param(value=0)
g = m.Param(value = 3.69)                    #Gravity on Mars (m/s^2)
mu = m.Param(value = 0.65)                    #Friction Coefficient
C_f = m.Param(value = 1.1)                    #Motor casing loss coefficient
m_r = m.Param(value = 350)                    #Mass (kg)
n_w = m.Param(value = 6)                      #Number of wheels
alpha_d = m.Param(value = 30)                 #Max slope angle
pi = m.Param(value = np.pi)                   #Pi
n = m.Param(value = 1.0)                      #Soil deformation index
k_c = m.Param(value = 0.1)                    #Soil cohesive modulus
k_phi = m.Param(value = 3.9)                  #Soil friction modulus

theta_d = m.Param(value = 90)
theta = m.Intermediate(theta_d*pi/180)

omega_m, r_w, V_max, t_a, N_gr, b_w  = [m.Var() for i in range(6)]


omega_m.UPPER = 6000
omega_m.VALUE = 3500
omega_m.LOWER = 2500

r_w.UPPER = 0.35
r_w.VALUE = 0.30
r_w.LOWER = 0.25

b_w.UPPER = 0.30
b_w.VALUE = 0.22
b_w.LOWER = 0.20


V_max.UPPER = 0.5
V_max.VALUE = 0.2
V_max.LOWER = 0.1


t_a.UPPER = 4
t_a.VALUE = 0.5
t_a.LOWER = 0.1
```

```
N_gr.UPPER = 100
N_gr.VALUE = 20
N_gr.LOWER = 10

alpha = m.Intermediate(alpha_d*pi/180)              #Max slope angle in radians
m_w = m.Intermediate(m_r/n_w)                       #Mass acting on each wheel

RR = m.Intermediate(m_r*mu)                         #Rolling resistance
GR = m.Intermediate(m_r*m.sin(alpha))               #Grading resistance
F_a = m.Intermediate(m_r*V_max/(g*t_a))             #Acceleration force

z_rw = m.Intermediate((3*(m_w*g)*m.cos(alpha)/((3-n)*(k_c + b_w*k_phi)*m.sqrt(2*r_w)))**(2/(2*n+1)))

#F_Rc = m.Intermediate((1/g)*b_w*((z_rw**(n+1))/(n+1))*(k_c/b_w + k_phi)) #Compacting force

TTE = m.Intermediate(RR + GR + F_a)                 #Total Tractive Effort
T_wnet = m.Intermediate(1.0*TTE*C_f*r_w)            #Net wheel torque
T_w = m.Intermediate(T_wnet/n_w)



T_mnet = m.Intermediate(T_wnet/N_gr)                #Total Motor Torque
T_m = m.Intermediate(T_mnet/n_w)                    #Torque per Motor
P_m = m.Intermediate(T_m*omega_m*0.10472)
up_slip = m.Intermediate((1-V_max/(r_w*omega_m*0.10472/N_gr)))
F_x = m.Intermediate(m_w*m.sin(alpha)*m.sin(theta))
eta = m.Intermediate(F_x*r_w*(1-up_slip)/T_w)


#Equations
m.Equation(up_slip**2 < 0.6)
#m.Equation(eta > 0.2)
m.Equation(P_m == 60)

#Objectives
m.Minimize(P_m) #Minimize Motor Power
# m.Maximize(alpha)
m.Minimize(r_w)
m.Minimize(t_a)


m.Maximize(eta)
#m.Maximize(V_max)
#m.Minimize(V_max)

m.Minimize(up_slip**2)
#m.Minimize(N_gr)

#m.Minimize()

m.Minimize(z_rw)
#m.Minimize(F_Rc)

#Set global options
m.options.IMODE = 3 #steady state optimization
```

```
#Solve simulation
#m.open_folder()
m.solve(disp=True)

#Results
print('')
print('Results')
print('Rover Mass:' + str(m_r.VALUE))
print('Rover top speed (m/s): ' + str(V_max.value))
print('Max angle:' + str(np.rad2deg(alpha.VALUE[0])))
print('Acceleration time (s): ' + str(t_a.value))
print('Wheel radius (m): ' + str(r_w.value))
print('Wheel width (m): ' + str(b_w.value))
print('Motor RPM:' + str(omega_m.value))
print('Gear Ratio:' + str(N_gr.value))
print('Motor Torque (Nm):' + str(T_m.VALUE))
print('Motor Power (W):' + str(P_m.VALUE))
print('Total Wheel Torque:' + str(T_wnet.VALUE))
print('Individual Wheel Torque:' + str(T_w.VALUE))
print('Total Torque Available:' + str(T_mnet.VALUE[0]*N_gr.VALUE[0]))
print('Slip Ratio:' + str(up_slip.VALUE))
#print('Rolling Resistance' + str(RR.VALUE[0]*g.VALUE[0]*V_max.VALUE[0]))
#print('Sinkage:' + str(z_rw.VALUE))
print('Tractive Efficiency (%):' + str(eta.VALUE[0]*100))
#print('Total Torque (Nm):' + str(T_w.VALUE))
```

Scout Bot

```
from gekko import GEKKO
import numpy as np

#Initialize model
m = GEKKO(remote=False)

#define parameter
eq = m.Param(value=0)
g = m.Param(value = 3.69)                  #Gravity on Mars (m/s^2)
mu = m.Param(value = 0.65)                  #Friction Coefficient
C_f = m.Param(value = 1.1)                  #Motor casing loss coefficient
m_r = m.Param(value = 120)                  #Mass (kg)
n_w = m.Param(value = 2)                    #Number of wheels
alpha_d = m.Param(value = 30)               #Max slope angle
pi = m.Param(value = np.pi)                 #Pi
n = m.Param(value = 1.0)                    #Soil deformation index
k_c = m.Param(value = 0.1)                  #Soil cohesive modulus
k_phi = m.Param(value = 3.9)                #Soil friction modulus

theta_d = m.Param(value = 90)
theta = m.Intermediate(theta_d*pi/180)

omega_m, r_w, V_max, t_a, N_gr, b_w  = [m.Var() for i in range(6)]


omega_m.UPPER = 6000
omega_m.VALUE = 3500
omega_m.LOWER = 2000
```

```
r_w.UPPER = 0.50
r_w.VALUE = 0.45
r_w.LOWER = 0.40

b_w.UPPER = 0.30
b_w.VALUE = 0.22
b_w.LOWER = 0.20


V_max.UPPER = 1.5
V_max.VALUE = 1.5
V_max.LOWER = 1.0


t_a.UPPER = 1.5
t_a.VALUE = 0.5
t_a.LOWER = 0.1

N_gr.UPPER = 100
N_gr.VALUE = 20
N_gr.LOWER = 10

alpha = m.Intermediate(alpha_d*pi/180)              #Max slope angle in radians
m_w = m.Intermediate(m_r/n_w)                       #Mass acting on each wheel

RR = m.Intermediate(m_r*mu)                         #Rolling resistance
GR = m.Intermediate(m_r*m.sin(alpha))               #Grading resistance
F_a = m.Intermediate(m_r*V_max/(g*t_a))             #Acceleration force

z_rw = m.Intermediate((3*(m_w*g)*m.cos(alpha)/((3-n)*(k_c + b_w*k_phi)*m.sqrt(2*r_w)))**(2/(2*n+1)))

#F_Rc = m.Intermediate((1/g)*b_w*((z_rw**(n+1))/(n+1))*(k_c/b_w + k_phi)) #Compacting force

TTE = m.Intermediate(RR + GR + F_a)                 #Total Tractive Effort
T_wnet = m.Intermediate(1.0*TTE*C_f*r_w)                    #Net wheel torque
T_w = m.Intermediate(T_wnet/n_w)



T_mnet = m.Intermediate(T_wnet/N_gr)                #Total Motor Torque
T_m = m.Intermediate(T_mnet/n_w)                    #Torque per Motor
P_m = m.Intermediate(T_m*omega_m*0.10472)
up_slip = m.Intermediate((1-V_max/(r_w*omega_m*0.10472/N_gr)))
F_x = m.Intermediate(m_w*m.sin(alpha)*m.sin(theta))
eta = m.Intermediate(F_x*r_w*(1-up_slip)/T_w)


#Equations
m.Equation(up_slip**2 < 0.8)
#m.Equation(eta > 0.2)
m.Equation(P_m == 95)

#Objectives
m.Minimize(P_m) #Minimize Motor Power
```

```
m.Minimize(t_a)


m.Maximize(eta)
m.Maximize(V_max)


m.Minimize(up_slip**2)
#m.Minimize(N_gr)

#m.Minimize()

m.Minimize(z_rw)
#m.Minimize(F_Rc)

#Set global options
m.options.IMODE = 3 #steady state optimization

#Solve simulation
#m.open_folder()
m.solve(disp=True)

#Results
print('')
print('Results')
print('Rover Mass:' + str(m_r.VALUE))
print('Rover top speed (m/s): ' + str(V_max.value))
print('Max angle:' + str(np.rad2deg(alpha.VALUE[0])))
print('Acceleration time (s): ' + str(t_a.value))
print('Wheel radius (m): ' + str(r_w.value))
print('Wheel width (m): ' + str(b_w.value))
print('Motor RPM:' + str(omega_m.value))
print('Gear Ratio:' + str(N_gr.value))
print('Motor Torque (Nm):' + str(T_m.VALUE))
print('Motor Power (W):' + str(P_m.VALUE))
print('Total Wheel Torque:' + str(T_wnet.VALUE))
print('Individual Wheel Torque:' + str(T_w.VALUE))
print('Total Torque Available:' + str(T_mnet.VALUE[0]*N_gr.VALUE[0]))
print('Slip Ratio:' + str(up_slip.VALUE))
#print('Rolling Resistance' + str(RR.VALUE[0]*g.VALUE[0]*V_max.VALUE[0]))
#print('Sinkage:' + str(z_rw.VALUE))
print('Tractive Efficiency (%):' + str(eta.VALUE[0]*100))
#print('Total Torque (Nm):' + str(T_w.VALUE))
```

A2. Internal Science mechanism components

Gantry: A gantry system is attached to the top of the science module and covers a working volume of 610 mm × 460 mm × 200 mm. For transporting test tubes or cuvettes, a 2 fingered end effector controlled by a motor, is used to hold them from the top. Lead screws which rotate with the help of motors enables the end effector of the gantry to move in 3 axes.

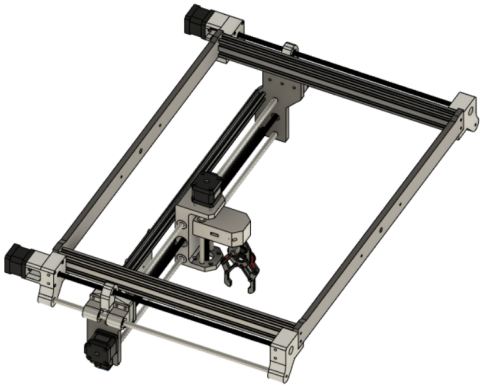

Gantry

Conveyor belt

Conveyor belt: Linear conveyor belts with test-tube and cuvette holders are used to transport the cuvettes beyond the working area of the gantry. There are 3 conveyor belts present within the science module, and each of them is controlled by a motor capable of reversing its motion. The cuvettes and test tubes are placed on a stand attached to the conveyor surface to ensure that they do not topple over.

Test tube and Cuvette storage: The test tubes are 20 mm in diameter and 150 mm in length and made of Titanium with lead coating on the inside (APXS requires lead shielding). The cuvettes have a square base of the edge length of 12 mm and would be 45 mm high and made of Sapphire to ensure durability. The cuvettes have an additional attachment made of Titanium at the top to increase its protection and ensure the arm can pick it up without much difficulty.

The storage has a cavity to reduce weight and double as a storage section, such as for electronic components. The storage base is fitted with 4 Neodymium magnets on each corner (1.26"

diameter and 0.06" thickness). The

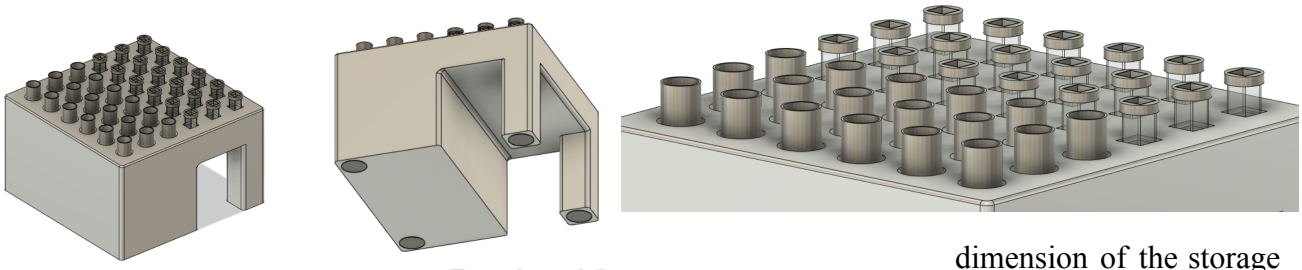

Test tube and Cuvette storage

dimension of the storage compartment is 260 mm × 260 mm × 170.524 mm.

Lid placement system:

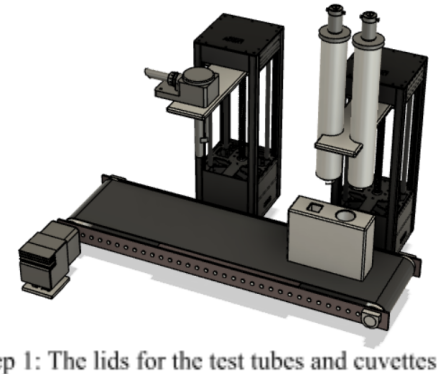

Step 1: The lids for the test tubes and cuvettes are stored on helixes in 2 vertical tubes. These 2 tubes are c linear actuator which can move verti

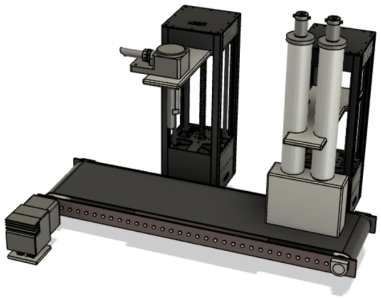

Step 2: The linear actuator moves down, and at the same time the helix rotates such that the lid is placed precisely on the e. After this, the linear actuator moves down it to ensure that the lid is properly placed.

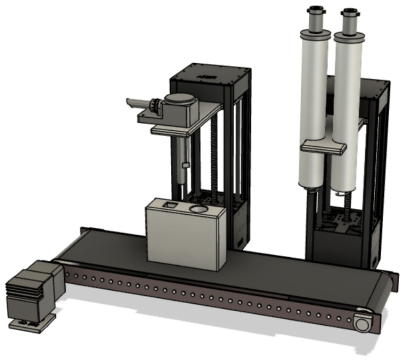

Step 3: Once done, the conveyor reverses motion and moves the test tube and cuvette to the sealing area where the test tubes are sealed. The sealing is done with the help of a shape memory alloy.

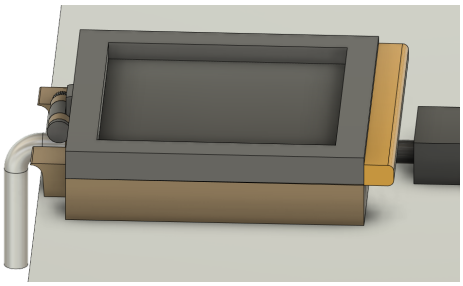

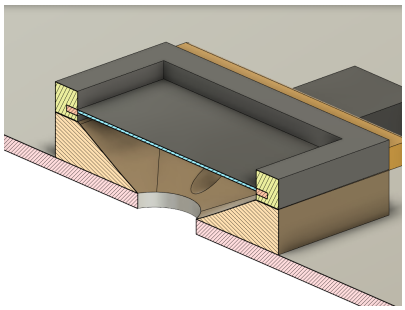

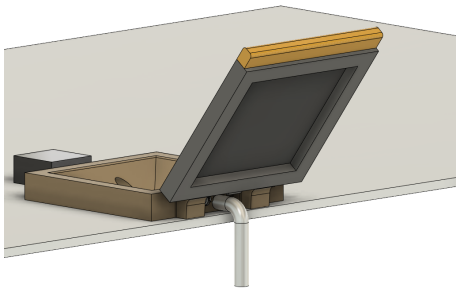

Soil filtration:

Step 1: The robotic arm disposes the collected soil In the filter.

Step 2: The sieve is agitated by an internal mechanism present inside the top lid.

Step 3: The remaining sediments would be disposed of by the rotary action of the motor.

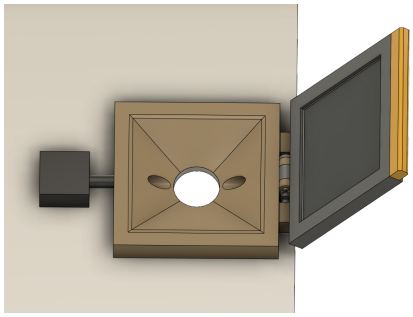

Step 4: After deposition, the aperture below and the sieve above would close, and the airjet will blow out the remaining contaminants.

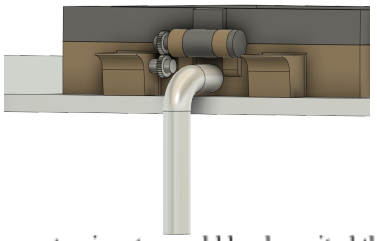

Step 5: The contaminants would be deposited through the pipe which runs along the outer edge of the chassis. The motor casing doubles as a support so that the sieve doesn't hit the pipe directly.

Raman spectroscopy mechanism:

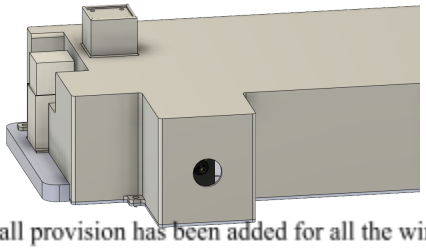

A small provision has been added for all the wirings present in the device.

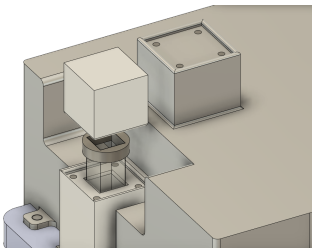

The lid would be removed and placed upon the temporary holder atop the outer cover by the end effector. The base of the cuvette holder, temporary holder and cuvette lid are fit with magnets to ensure the lid doesn't topple off during transit.

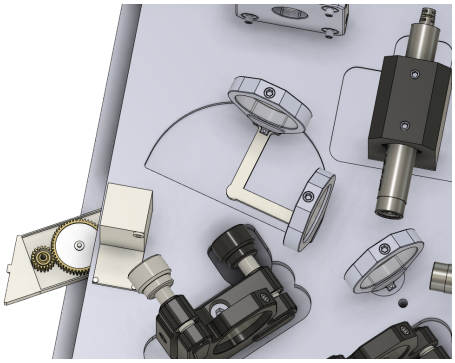

Gears are assembled inside a small sliding slot which would connect with the motor and the right angle filter holder in order to switch the filters according to the laser being used.

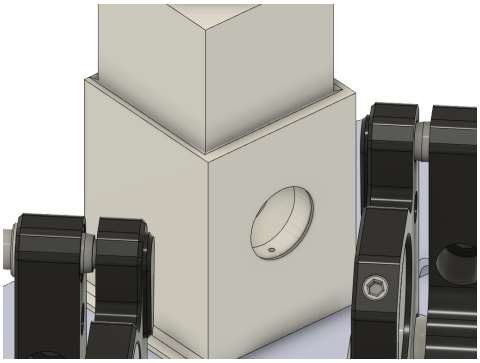

A small provision has been made for a screw to hold the focusing lens in place.

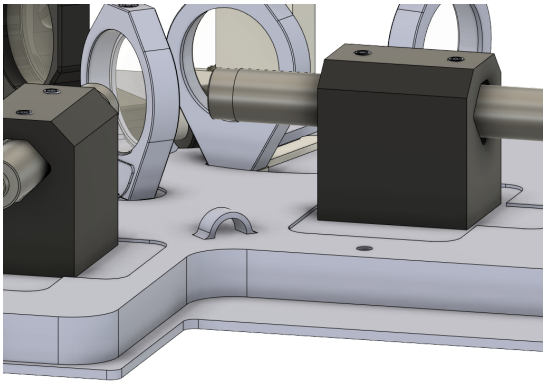

Small provisions are provided for wires from the motor to be re routed to the circular exit.

APXS test mechanism:

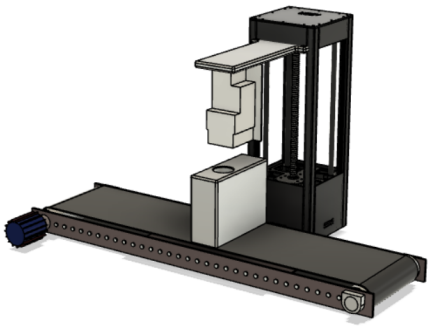

Step 1: The conveyor moves the test tube to the APXS device which is attached to the end of a linear actuator.

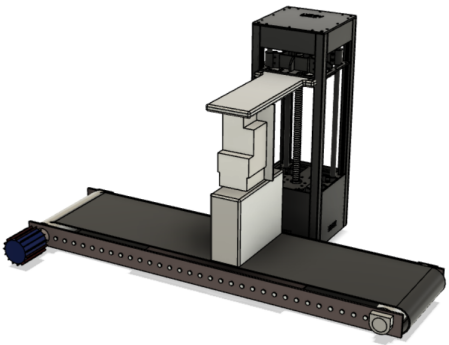

Step 2: The linear actuator lowers the APXS device onto the mouth of the test tube, and the test is conducted.

ATP bioluminescence test mechanism:

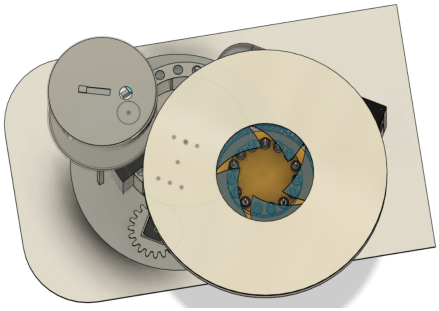

The swab dispenser releases the swab for the gripper to use to take a sample. The swab has a magnetic cap at the at the end which would be used to close the luminometer assembly shown below

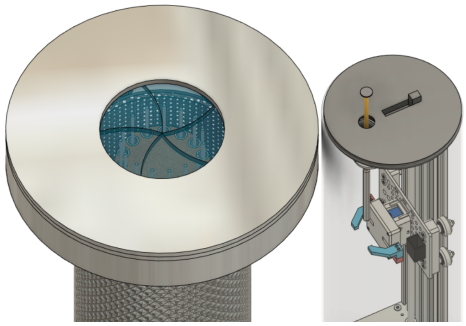

After the robotic arm takes a sample with the swab, it is placed into the airlock. Here inside the airlock it is then transported by an end effector along with the end effector is an isotopic heating unit which would help resist the change in equilibrium temperature of the testing chamber.

A gripper transports the swab through the airlock to get it to the testing assembly.

The testing area is readied by the reagent dispenser. Which releases the enzymes into the testing tube before swab is dropped in. The dispenser works by using a linear actuator to lower the reagent pipes into the tube to avoid spillage.

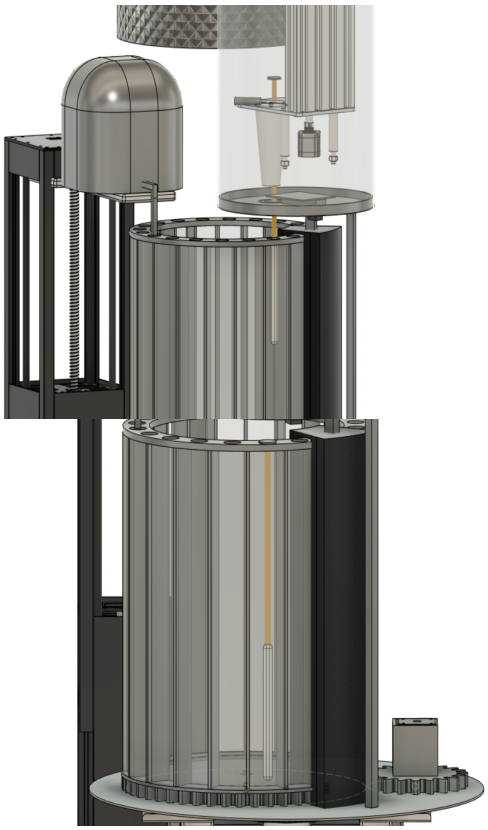

The swab is dropped into the readied tube. The magnetic clamp of the swab prevents it from shaking and disrupting the test. After this it moves into the sliding luminometer to be tested for bioluminescence.

Once the swab containing test tube is passe into the luminometer assembly , the test can be conducted. Darkness is ensured by this setup

A.3 Robotic Arm

A.3.1 Tool tray

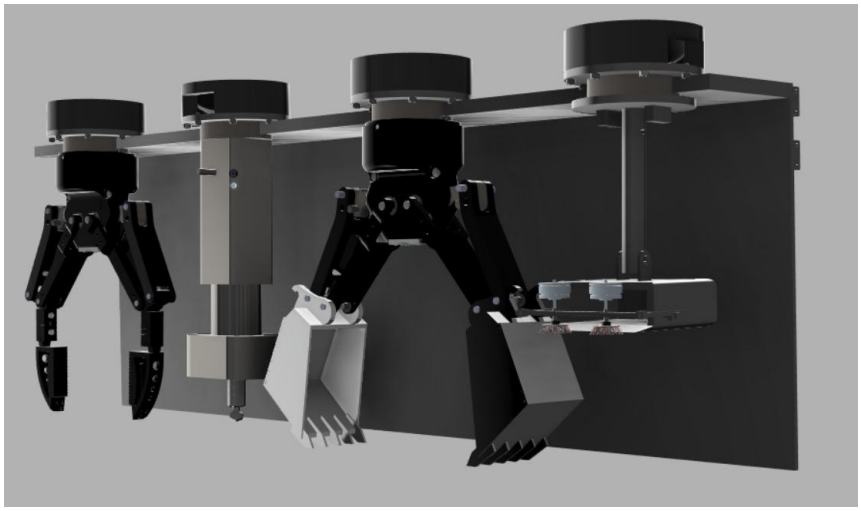

A.3.2 Custom made torque calculation script with torque calculations

CRISS ARM TORQUE ANALYSIS

The minimum criteria being the Arm does not fall under its own weight,for the arm being completely stretched out horizontally carrying the load

Load Capacity - M

Actuator weights - A1 , A2 , A3

link weight - W1 , W2 , W3

link Lengths - L1, L2 , L3

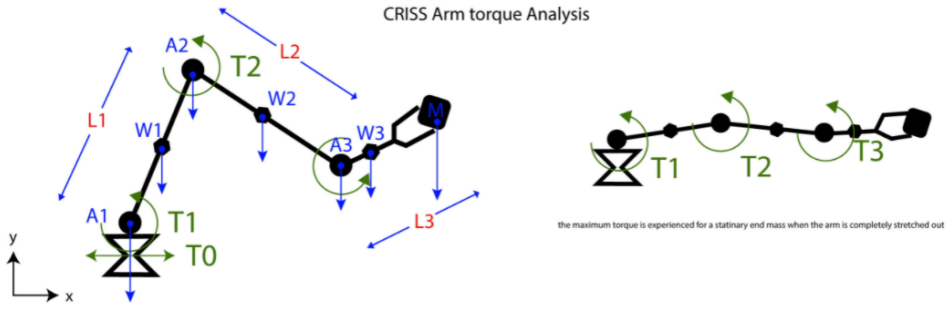

T0 only depends on the moment of inertia of the arm about y axis,since we are considering a stationary arm we can neglect T0

```
[1] #Enter the Arm Parameters
    g= 3.711
    M=float(input("Enter value of M in kg:"))
    A1,A2,A3=float(input("Enter the Value of A1(in kg)0:")),float(input("Enter the Value of A2(in kg):")),float(input("Enter the Value of A3(in kg):"))
    W1,W2,W3=float(input("Enter the Value of W1(in kg):")),float(input("Enter the Value of W2(in kg):")),float(input("Enter the Value of W3(in kg):"))
    L1,L2,L3=float(input("Enter the Value of L1(in m):")),float(input("Enter the Value of L2(in m):")),float(input("Enter the Value of L3(in m):"))

    #ALL MASSESS ARE IN KG , *3.711 at the end for convertion to N
```

```
Enter value of M in kg:3
Enter the Value of A1(in kg)0:6
Enter the Value of A2(in kg):3
Enter the Value of A3(in kg):6
Enter the Value of W1(in kg):0.87
Enter the Value of W2(in kg):0.7
Enter the Value of W3(in kg):1.5
Enter the Value of L1(in m):0.5
Enter the Value of L2(in m):0.4
Enter the Value of L3(in m):0.3
```

```
[3] # Torque analysis for maximum statinary condition i.e. theta1=theta2=theta3=0

    T3 = ((W3*L3/2)+(M*L3))*g
    T2 = ((W2*L2/2)+(A3*L2)+(W3*(L2+L3/2))+(M*(L3+L2)))*g
    T1 = ((W1*L1/2)+(A2*L1)+(W2*(L1+L2/2))+(A3*(L1+L2))+(W3*(L1+L2+L3/2))+M*(L1+L2+L3))*g
    print("T3 = ",round(T3),"Nm")
    print("T3 = ",round(T2),"Nm")
    print("T1 = ",round(T1),"Nm")
```

```
T3 =  4 Nm
T3 =  20 Nm
T1 =  47 Nm
```

A.3.3 Structural Analysis of Links

Ultimate Tensile strength-9.3 x 10^8 Pa

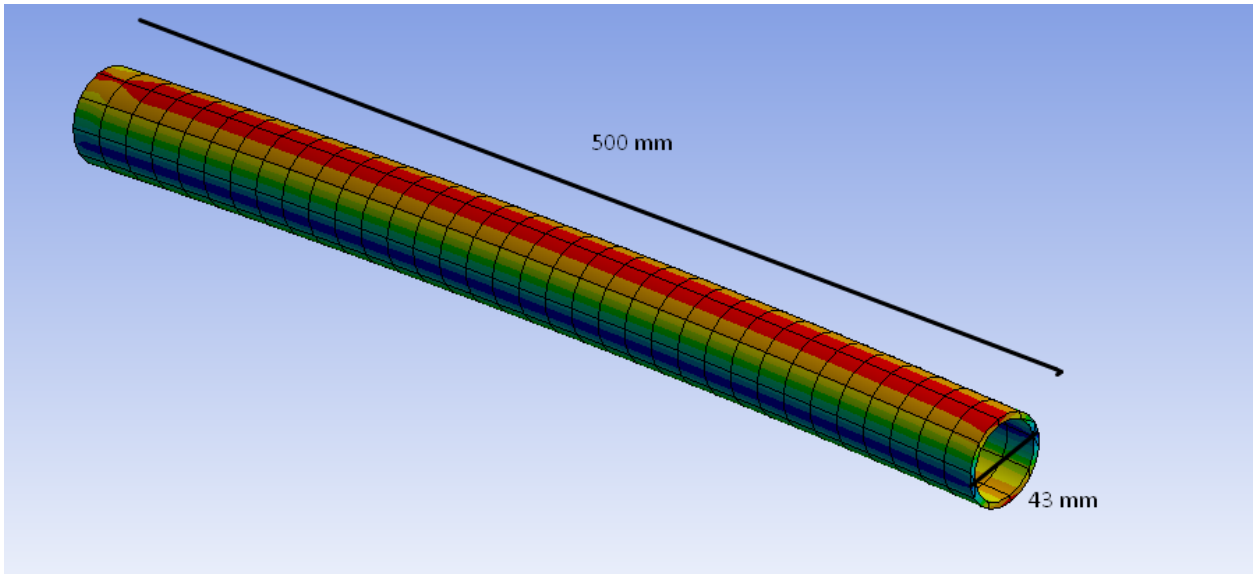

Link 1- Structural Analysis

Max vonMises Stress-2.26 x 10^7 Pa

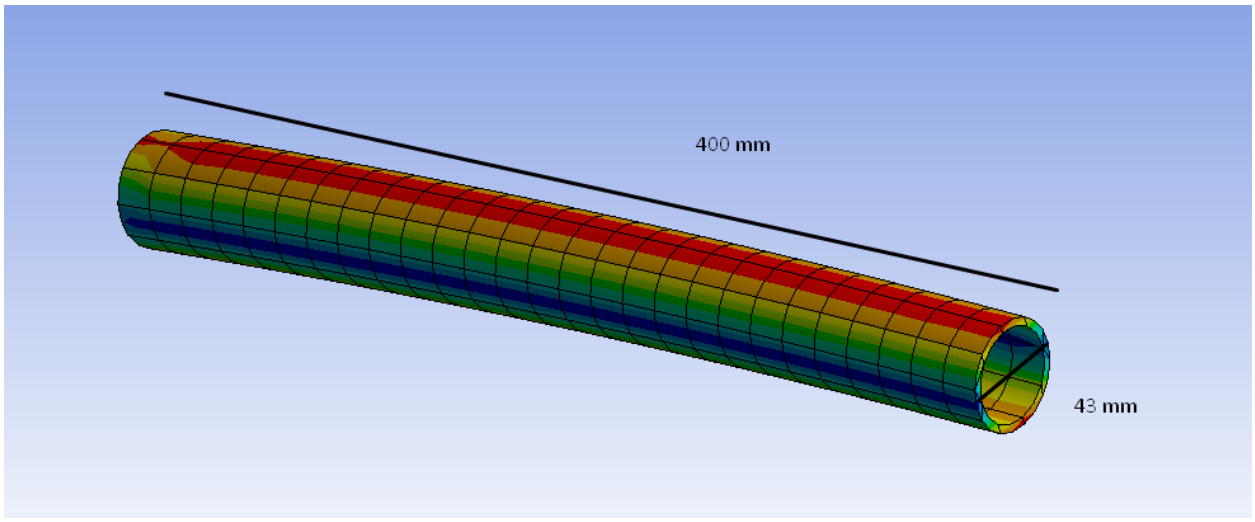

Link 2-Structural Analysis

Max vonMises Stress-2.11 x 10^7 Pa

A.3.4 Joint with harmonic gearbox exploded view

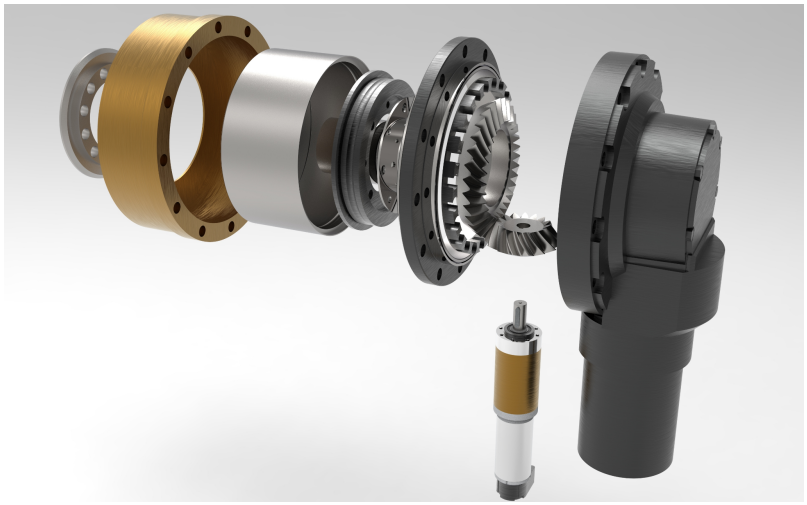

A.3.5 Arm Retraction

Appendix B: Electrical

B1. Powers

B.1.1 Block diagram of the power systems architecture of the

(a) Science bot

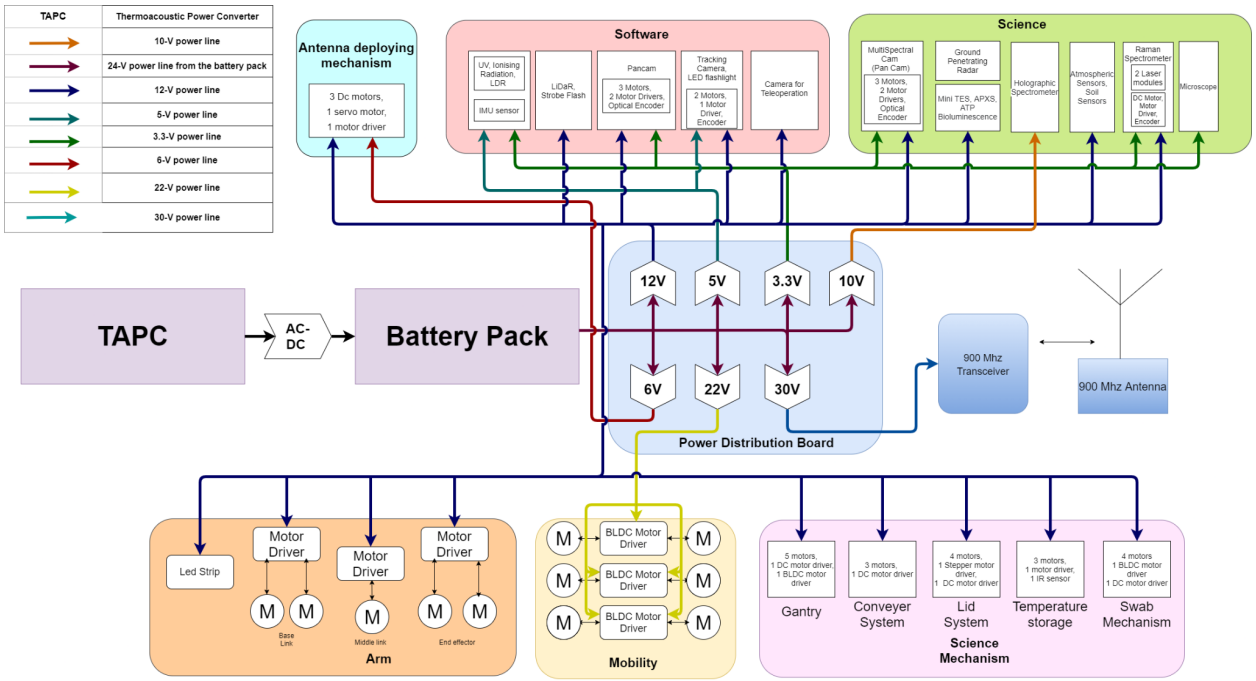

(b) Scout bot

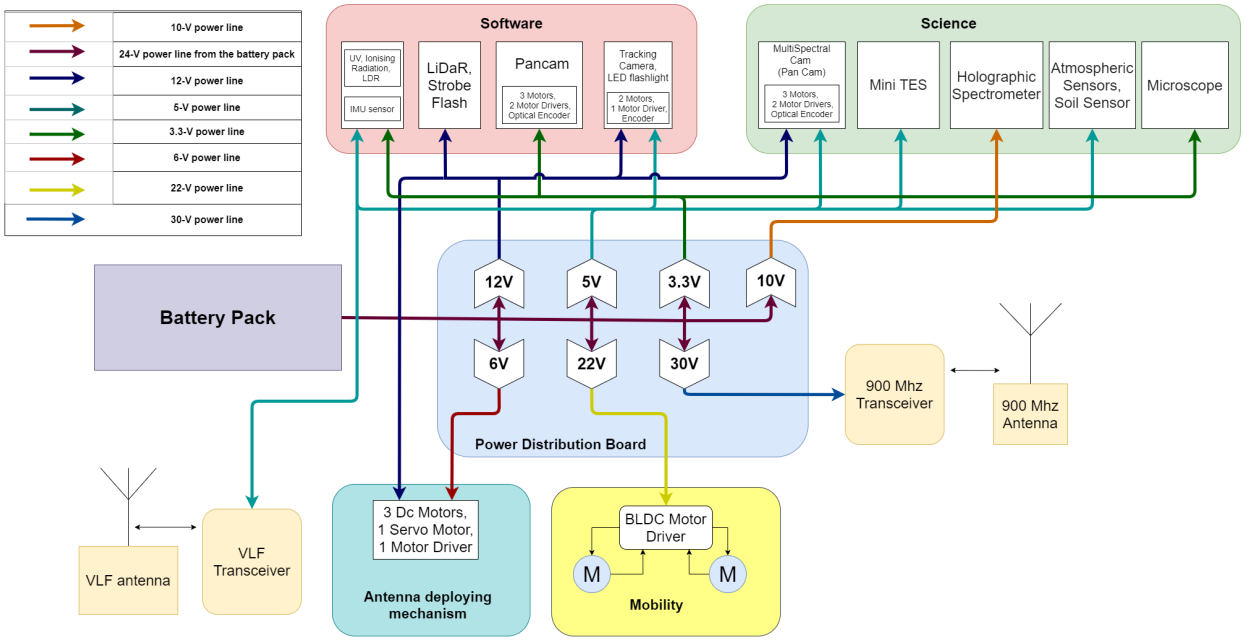

B.1.2: Considerations made other than TAPC for recharging the batteries on the science rover:

Multi Mission radioisotope generator: MMRTG is a radioisotope generator used by NASA in the Curiosity rover. It works on the principle of converting thermal energy into electrical energy through thermocouples. It uses 8 general purpose heat source modules as its thermal power source. It weighs around 43 kg and has an electrical output of 145 Watt in the beginning of life.

This was not used in our design because it has very low specific electrical power of around 3.4 Watt per kg.[2.24]

Advanced Stirling Radioisotope generator: It is a generator which works on stirling thermodynamic cycle and converts heat energy into kinetic energy by moving the pistons and kinetic energy into electrical energy by inducing current in a loop by moving magnets to and fro attached to the piton. It uses 2 general purpose heat sources as its power source. It weighs around 32 kg and has an electrical power output of 130 Watts in the beginning of life. This was not used in our design because it has a specific electrical power of 4.1 Watt per kg which is much lower than TAPC and it also has high exported vibration of around 2 Newtons which is much higher than 0.2 Newtons of TAPC.[2.25, 2.26]

Science Bot - Moving

Science Bot			
Science - Mechanism		Science	
Component	Power Required (In Watts)	Component	Power Required (In Watts)
Temperature Storage	10.8	Alpha Particle X Ray Spectrometer	2
Conveyor System	7.2	Pancam	9.2
Gantry	18	Luminometer	0
Raman Spectroscopy	3.6	Mini TES	5.4
Lid System	14.4	Lasers	1.25
Swab Mechanism	14.4	Blackfly S GigE	3
Tracking Camera	7.2	FPGA Circuit	0.03
Pancam Motors	10.8	CCD Sensor	0.075
Total - 86.4		Toy Motor	2.25
		Sensors	5
		Led Light	3.3
		Total - 31.505	

Software		Communications	
Component	Power Required (In Watts)	Component	Power Required (In Watts)
Lidar	90	Servo Motor	9.6
Tracking camera	1.5	Spur Geared Motor	10.8
LED Light	40	Antenna	30
Flash Light	50	Repeaters	2
Telemetry Camera	3	Total - 50.4	
Total - 184.5			
Arm		Mobility	
Component	Power Required (In Watts)	Component	Power Required (In Watts)
Brushed Dc Motor	420.864	Brushed Dc Motor	360
Embedded Science			
Component	Power Required (In Watts)		
OBC	40		
Sensors	5		
Total - 45			

Scout Bot			
Software		Science	
Component	Power Required (In Watts)	Component	Power Required (In Watts)
Tracking camera	1.5	Pancam	20
Flash Light	50	Mini TES	5.4
LED Light	40	CCD Sensor	0.075
Flash Light	50	Toy Motor	2.25
Telemetry Camera	3	Sensors	5
Total - 184.5		Lasers	1.25
		Microscope	3.5
		Total - 37.475	
Embedded Science		Mobility	
Component	Power Required (In Watts)	Component	Power Required (In Watts)
OBC	80	Brushed Dc Motor	360
Sensors	5		
Total - 85			
Communications			
Component	Power Required (In Watts)		
Servo Motor	9.6		
Spur Geared Motor	10.8		
Antenna	30		
Repeaters	2		
VLF	1		
Total - 51.4			

Science - Mobility	
Subsystem	Power Required(in Watts)
Software	181.5
Science	28.205
Mobility	360
Science - Mechanism	86.4
Communications	51.4
Embedded	45
Total - 752.505	

Science - Arms	
Subsystem	Power Required(in Watts)
Software	181.5
Science	28.205
Arm	420
Science - Mechanism	86.4
Communications	51.4
Embedded	45
Total -812.505	

Scout Bot	
Subsystem	Power Required(in Watts)
Software	181.5
Science	26.205
Mobility	180
Communications	51.4
Embedded	85

Total - 524.105

B2. Controls

B.2.1: Block diagrams

Block diagram of the embedded systems architecture of the

(a) Scout bot

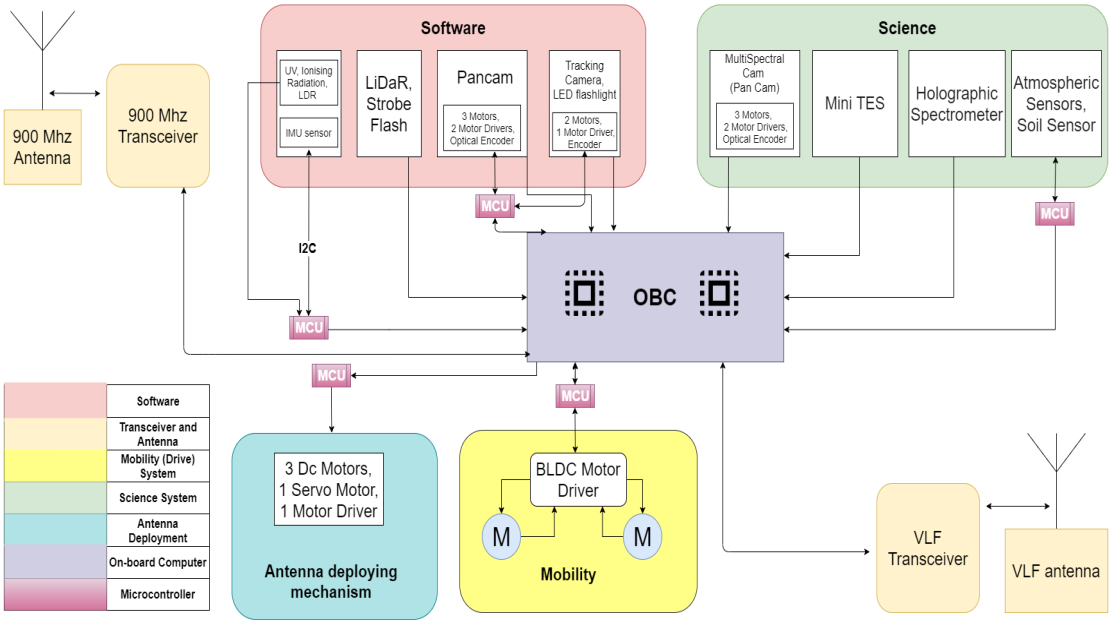

(b) Science bot

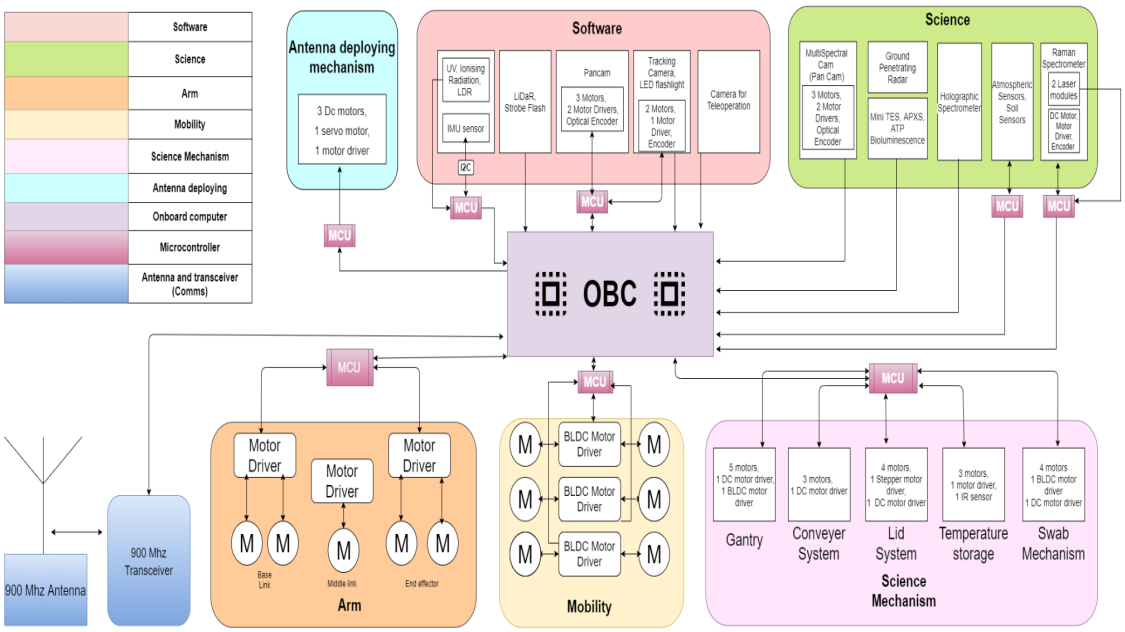

* A CAN bus was implemented for the intra rover communication

B.2.2: Table of motors

Subteam	Motor	No.	Torque (Nm)	Speed (rpm)/ step size	Voltage (V)	Current (A)
Arm	Brushed Gear motor	6	14.72	29	10.24 (operating)	6.85(Operating)
Gantry	Brushless DC	4	0.8	10	12	0.5
	Spur geared motor	1	0.7	10	12	0.3
Conveyor system	Spur geared motor	2	0.7	10	12	0.3
Temperature storage	Brushed DC	2	0.5	10	12	0.3
	Spur geared motor	1	0.7	10	12	0.3
Lid System	stepper motor	3	0.03	1.8 degree	12	0.3
	Brushed DC	1	0.5	10	12	0.3
Swab Mechanism	Spur geared motor	2	0.7	10	12	0.3
	Brushed DC	1	0.5	10	12	0.3
	Brushless DC	1	0.8	10	12	0.5

Raman Spectroscopy	Brushed DC	1	0.3	5	12	0.3
Tracking Cam rotation	Brushed DC	2	0.3	5	12	0.3
Pan Cam	Brushed DC	3	0.3	5	12	0.3
Mobility - Science Rover	Brushless DC Motor	6	22.6	2500~3000	22	1~3
Mobility - Scout Bot	Brushless DC Motor	2	45.2	2000	22	1.6~4.3
Antenna deployment mechanism	Servo motor	1	2	40	4.8 to 6	1.6
	Spur geared motor	3	0.7	10	12	0.3

Motors: For arm, Brushless DC motor-DCX35 GBKL from maxon motors along with compatible 83:1 gearbox and 1024 counts per turn encoder was used. For the drive systems, F-N100R-02 and D-N100R-02 brushless DC linear actuators were used for scout and science bots respectively.

B.2.3: Main Computer specs

Specification	**Science**	**Scout**
GPU	512-core	1024-core
CPU	8-core, 12 MB cache 64-bit ARM	16-core, 24 MB cache 64-bit ARM

The systems also contain DL accelerators, Vision accelerators, and units specialized for H.265 and H.266 codecs. Furthermore, the system also has all the peripherals necessary for interfacing with the rest of the system

B3. Communications

B.3.1: Block diagram

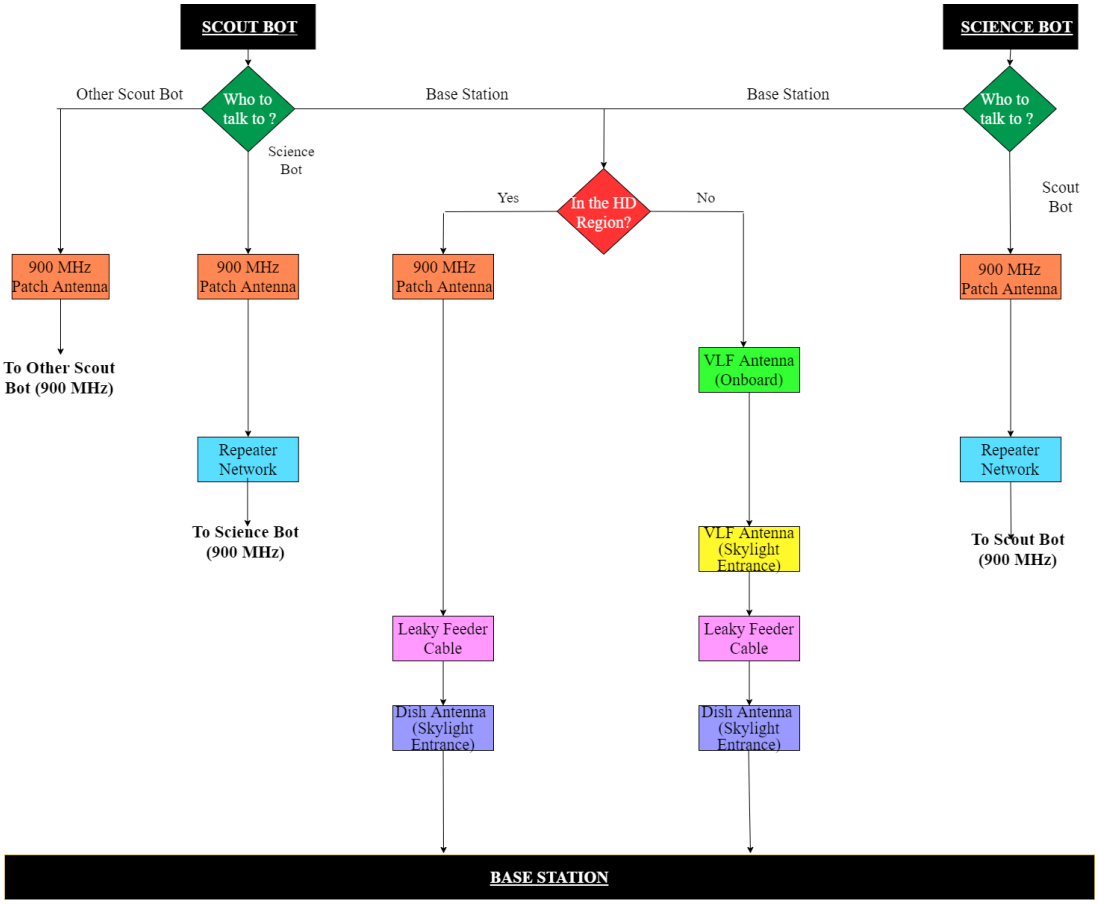

B.3.2: Link Budget

	Repeater-Repeater	**Scout-Scout**	**Leaky Feeder - Repeater**	**Skylight - Base station**
Frequency	900 MHz	900 Mhz	900 Mhz	433 MHz
Transmit Power	30 dBm	45 dBm	30 dBm	45 dBm
Transmitter Gain	10 dB	15 dB	10 dB	10 dB
Distance	100 m	400 m	200 m	5 km
FSPL	72 dB	84 dB	84 dB	99 dB
NLOS	33 dB	60 dB	30 dB	30 dB
Receiver Gain	10 dB	15 dB	15 dB	15 dB
Sensitivity of	-130 dB	-130 dB	-130 dB	-130 dB

Receiver				
Thermal Noise	-130 dB	-130 dB	-130 dB	-130 dB
Random Loss* **	30 dB	30 dB	30 dB	30 dB
Error correction	10 dB	10 dB	10 dB	10 dB
Link margin	22 dB	11 dB	22 dB	23 dB
Bandwidth	20 MHz	20 MHz	20 MHz	20 MHz
Code Rate	0.5	0.5	0.5	0.5
SNR	158.493	12.589	158.493	199.5262315
Shannon Limit	146 Mbps	75 Mbps	146 Mbps	153 Mbps
Payload Shannon Limit	73 Mbps	38 Mbps	73 Mbps	77 Mbps
60% Shannon Limit	44 Mbps	23 Mbps	44 Mbps	46 Mbps

*** Random loss includes- cable loss, impedance mismatch loss, implementation loss, polarization loss

B.3.3: Data Table

B.3.3.1: High bandwidth messages

Message type	**Source**	**Destination**	**Description**	**Size(Typ.)(Bytes)**	**Rate (Hz)**	**Priority**
Point cloud	5 sources (4 scouts + 1 science)	Base station andor scout bot	Mapping	3 (4.8*5) Mbytes	1	1
Live video	Science Bot	Base station	For teleoperation	0.25 Mbyte	1	2
Live Sensor data	5 sources (4 scouts + 1 science) [initially] and only Science bot[later]	Base station	Science Data	12.5 kByte	1	3

Telemetry data	Base station	Science Bot	Teleoperation data	0.125 kBytes	10	4

B.3.3.2: Low Bandwidth messages

Message type	**Source**	**Destination**	**Description**	**Size(Typ. In Bytes)**	**Rate (Hz)**	**Priority**
Region of interest Node	Scout bot	Base station	Coordinate of the region of interest and priority number of the site	16 Bytes	Whenever we find a region of interest	2
Robot status	5 sources (4 scouts + 1 science)	Base station	Robot ID ,Battery Power, Robot state, Time stamp	8 Bytes	Once in 5 seconds	1
Location	Scout bot	Base station	Current location of scout	12 Bytes	Once in 30 seconds	3

B.3.3.3: Inter bot comms(Mainly for scout-scout)

Message type	**Source**	**Destination**	**Description**	**Size(Typ. In Bytes)**	**Rate (Hz)**	**Priority**
Point cloud	5 sources (4 scouts + 1 science)	Scout - scout, scout-science	Single frame of point cloud data constituting 3 Mn points, in compressed form	24 Mbytes	1	1

B.3.3.4: Robot Status (Compressed Form)

Robot ID	**Battery Power**	**Robot state**	**Time stamp**
Robot ID encoded as a unique character- 1 Byte	Battery Power encoded as a unique character- 1 Byte	Robot state encoded as a unique character- 1 Byte	Time stamp consisting of 5 characters representing MMMSS

Appendix C: Software

C1:The rover considers the following factors to mark an area as a region of interest -

Entry/Exit points as well as skylight entrances are important regions of interest. In daytime, an optical sensor is mainly sufficient for detection, however at night time a combination of data from Lidar and Panoramic Camera is used to observe holes in the Lava tube ceiling. Apart from this, UltraViolet and Ionising radiation values, as well as gradients in the concentrations of atmospheric compounds, are compared to their values measured at the base link Skylight entrance. A unique method of comparing height gradients is used to differentiate between skylight entrances and openings. In the former case, the slope changes from positive to negative in case of piled debris on the ground, however in case of an opening, the value remains positive or settles to a small value after some distance. If an opening is detected the bot decides to return back to the cave for further exploration.

Life Detection:
In order to maximize the chances of detecting biosignatures, we aim to find sites with high exobiology potential. We will be looking for the sites that date back to Mars' early, life-friendly period, i.e., the Noachian to the Noachian/Hesperian boundary, or sites with subsurface ice, aqueous sediments, or minerals that can preserve organic biomarkers. Such sites can also contain minerals indicating past favorable conditions for liquid water or standing water, thermal spring environments, and the aqueous weathering processes. Sites containing minerals with high preservation potential for biosignatures, or minerals derived from elements essential for sustenance of life like sodium, magnesium, calcium also form the region of interest. Minerals such as olivine that are known to contain life in Mars analogous earth environments are also classified as potential sites for scientific analysis.

After minerals favorable to life are detected at a particular site, biological analysis is conducted. A promising biomarker for life detection can be defined as a chemical species or topographical pattern uniquely derived from living organisms and must not be synthesized abiotically, thus unambiguously indicating the presence of extinct or extant life. The biomarkers being detected by the science module have been put into three broad categories based on a priority order. The first priority consists of biomarkers belonging to a strictly biogenic origin, which are conclusive of extant and extinct lifeforms. The next priority level includes organic compounds, which come from both biotic and abiotic sources. It also includes minerals that are often produced as a result of biologically induced processes. The last priority level contains the biomarkers and minerals that do not have any biotic source yet can help understand the Martian conditions in detail. Refer Appendix D1.1. Based on the biomarkers and minerals detected at various priority levels by the science module, it can be determined how good the site is as a region of interest.

After the start of the mission, the scout bot will start streaming the live data from atmospheric sensors back to the base station. If any two of the atmospheric parameters are found to be within the threshold needed to support life(Appendix), it will flag the region and use its onboard instrumentation of PanCam and Mini TES for mineralogical analysis of the site. This data will also be transmitted to the science rover using an inter rover communication link. Using this data,

the science rover will mark the sites of interest and perform an in-depth analysis on the marked sites using its variety of onboard instruments. As the science bot will operate only in the high bandwidth region of 3kms, the data from the analysis and the location of sites will be sent back to the base station live.

When the scout bot crosses the 3 km mark and enters the low bandwidth region, it will cease the live stream of data from atmospheric sensors to the base station. The data will be stored on the rover, and any location where the atmospheric parameters cross a threshold value will be marked. The bot will collect soil samples by swabs on 40 of the most favorable marked locations on its return journey. It will also perform geological, and biomarker analysis using Panoramic Camera, Mini TES, and the Holographic Spectrometer on these sites and store the data.

In the Science bot, the high-resolution camera mounted at the top of the mast will provide color stereo pictures of the site, followed by Mini-TES providing remotely-sensed point discrimination of mineral composition of the terrain features. The texture, granularity, and other surface features of the points with high mineral content will be analyzed using the microscope mounted on the arm. The surface will also be analyzed for possible biofilms and microbial mats using the ATP Bioluminescence test. Ground-penetrating radar will provide information on the presence of the region's subsurface water, ice, and stratigraphic profile. This data will be stored in the onboard computer and will be processed in the base station to understand geological history, spatial heterogeneity, and the potential of origin and survival of life beneath the sub-surface. The site will then be drilled for the sampling of interior unoxidized surface or rock samples. The dust formed due to drilling will be collected using the soil collection mechanism name and transported to the Raman spectrometer cuvette, where it will be analyzed for potential biosignatures such as amino acids, lipids, sterols, hopanoids, and carbohydrates. It will be succeeded by elemental analysis through an Alpha Particle X-ray spectrometer. The drilled opening will also undergo an ATP bioluminescence test to detect traces of ATP. If co-occurring concentrations of biologically important molecules and minerals are detected or microscopic, and GPR analysis reveals heterogeneity suggestive of biological morphologies, the sample will be stored in the buffer box for further analysis at the base station.

On the basis of the biomarkers and minerals detected at various priority levels by the science module, it can be determined how favorable the site is as a region of interest. The **presence of water** is another great indicator of the possible presence of life. Living cells need liquid water for various biochemical processes. Hence, it is one of the most important factors for marking a region of interest. LIDAR will be used for surface water detection. Ground-penetrating radar will be used for subsurface water/ice detection. If a region with a flat terrain has atmospheric parameters (temperature, UV radiation, etc.) within certain threshold values that resemble Earth-like conditions and the science module has marked the region as a region of interest based on life detection parameters, then that site is also marked as a potential site for **habitability by humans** in the future.

High Magnetic fields indicate the presence of magnetic minerals in the surroundings, tracked by using a Magnetometer to identify such locations as a region of interest and collect data. Further analysis can be done based on the Image and Video data, and samples collected from these sites.

An image segmentation algorithm is going to be employed to identify **Unusual Geological structures**. Segmented image data fused with Lidar data will give us a reliable system for identifying unique rock structures. Similarly, a Deep Learning based rock and mineral classification model is also used to get an estimate of rock composition without performing heavy chemical and scientific testing on it. Finally, **trenches and big debris** which obstruct the path of our rover are a region of interest. This is because of two main reasons. Firstly, such massive obstructions in lava tubes can be an outcome of massive geological events, and provide information about the geological history of Martian Lava tubes. Secondly, as our rover cannot travel any further from the above-stated point, it is advisable to collect data from such points.

Appendix D: Science

D1. Prioritization of region of interests based on biomarkers, minerals and atmospheric parameters

<table>
<tr><th colspan="2">PRIORITY I</th></tr>
<tr><td>Organic Molecules</td><td>

DNA and RNA Bases:

Adenine
Guanine
Thymine
Cytosine
Uracil

Amino Acids :

Histidine

Lipids (Fatty Acids):

Stearic Acid
Palmitic Acid
Elaidic acid

Saccharides:

Monosaccharides - Arabinose, xylose, glucose, galactose and fructose
Disaccharides - Sucrose, Maltose, Lactose Trehalose
Trisaccharide - Raffinose

Pigments:

β Carotene
Chlorophyll
C-phycocyanin
Scytonemin

Hopanoids

17-α(H) 21 -β(H) opane

</td></tr>
<tr><td>Minerals</td><td>

Whewellite
Weddellite
Aragonite
Vaterite
Mellite

</td></tr>
<tr><td>Atmospheric Sensors</td><td>

Temperature (^{0}C): -15 to 115
Relative Humidity: 90%-100%
Pressure (MPa): 0.01-10
pH: 5-9

</td></tr>
<tr><td colspan="2">PRIORITY II</td></tr>
</table>

Organic Molecules	● **The enantiomeric excess of any amino acid.** ● **Carbonaceous Matter**
Minerals (which can preserve biomarkers and indicative of water chemistry)	● **Igneous minerals like olivine (Fo_{40} to Fo_{45})** ● **Pyroxenes:** 1. MgSiO3 2. FeSiO3 3. CaSiO3 ● **Oxides:** 1. Amorphous iron oxide 2. Ferrihydrite 3. Todorokite 4. Amorphous manganese oxide 5. Haematite ● **Carbonates:** 1. Calcite 2. Dolomite 3. Magnesite 4. Hydromagnesite ● **Phosphates:** 1. Hydroxyapatite 2. Calcium phosphate 3. Calcium pyrophosphate ● **Sulfates:** 1. Gypsum 2. Anhydrite 3. Anglesite 4. Barytes 5. Gypsum 6. Jarosites ● **Sulfides:** 1. Pyrite 2. Sphalerite 3. Galena ● **Opals**
Atmospheric Sensors	● **Temperature (^{0}C) <-15, >115** ● **Relative Humidity:** 80%-90% ● **Pressure (**MPa**)**: 0.02-0.01 ; 10-50 ● **pH:** 3-5 ; 9-11
PRIORITY III	
Atmospheric sensors	● **Temperature (^{0}C):** -1 ● **Relative Humidity:** 70%-80% ● **Pressure (**MPa**)**: 0.007-0.02 ; 50-111

	• **pH:** 0-3 ; 11-12.5

D2. Sensors used for atmospheric and soil analysis

Sensors	**Detection**
MG-811 Sensor	Carbon-dioxide
MQ-4	Methane
MQ-7	Carbon monoxide
Gravity I2C	Oxygen
MQ-135 Gas Sensor	NH3, NOx, Alcohol, Benzene, Smoke, CO2
SGAS707	Volatile Organic Compounds
DS18B20+	Temperature
DHT22 Digital Temperature and Humidity Sensor Module AM2302	Humidity and Temperature
GY-68 BMP180	Atmospheric Pressure
ML8511 UV Sensor	UV
X-Series detector	Ionizing Radiation
GY-273 HMC5883L Triple Axis Compass Magnetometer	Magnetic Field
7-in-1 Soil pH Meter	For measuring soil's pH, moisture, temperature, electrical conductivity, NPK concentration

FIELD MICROSCOPE

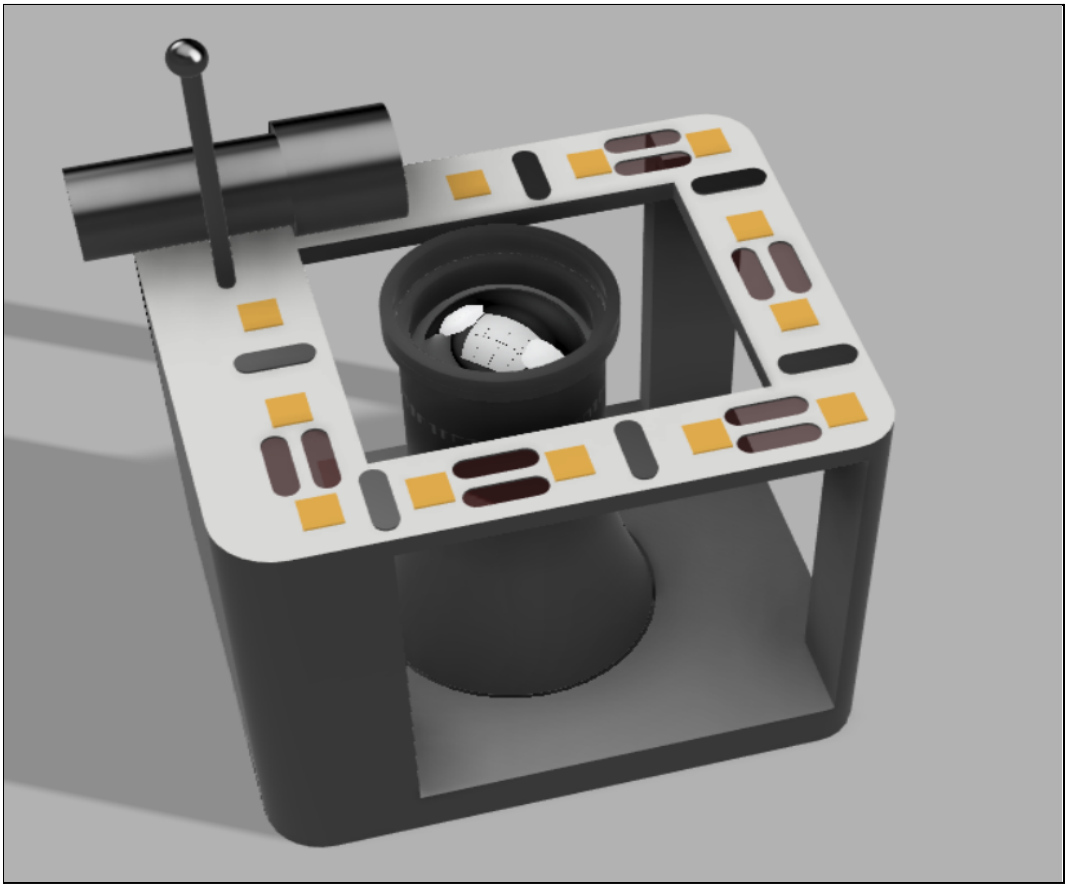

IONIZING RADIATION SENSOR

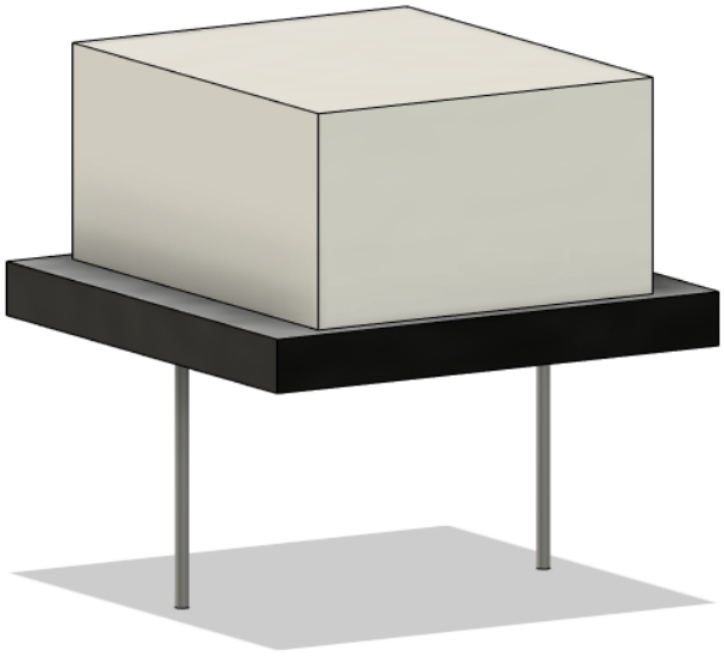

7-in-1 SOIL pH METER

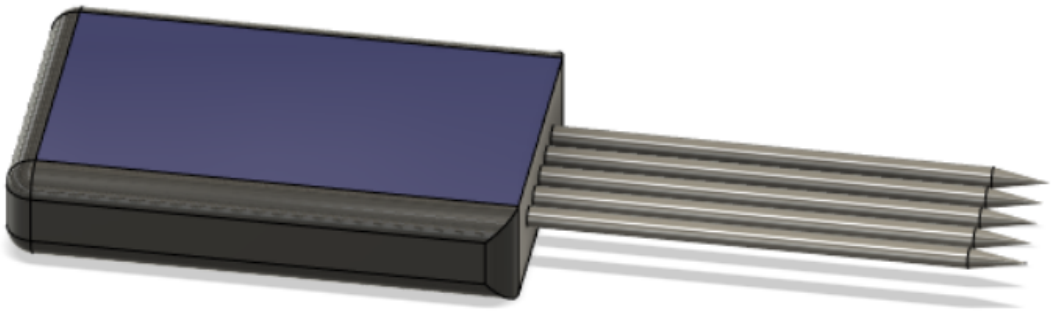

MQ-135 GAS SENSOR

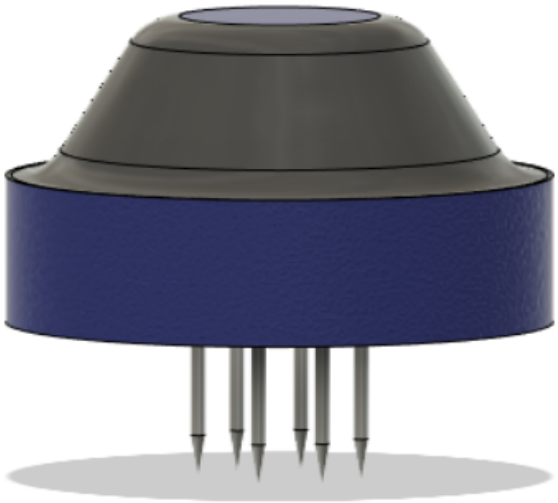

PANORAMIC CAMERA

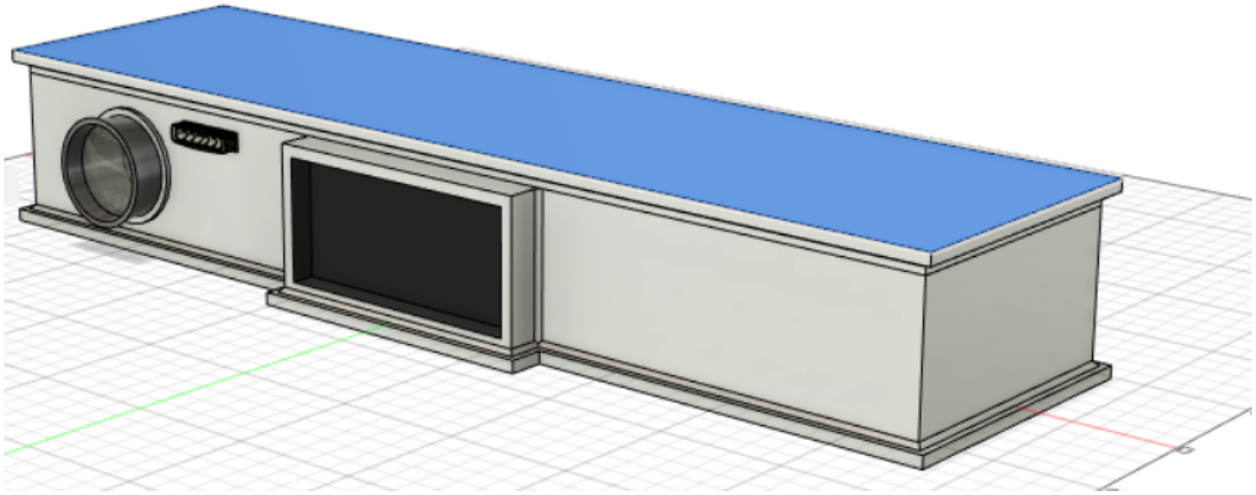

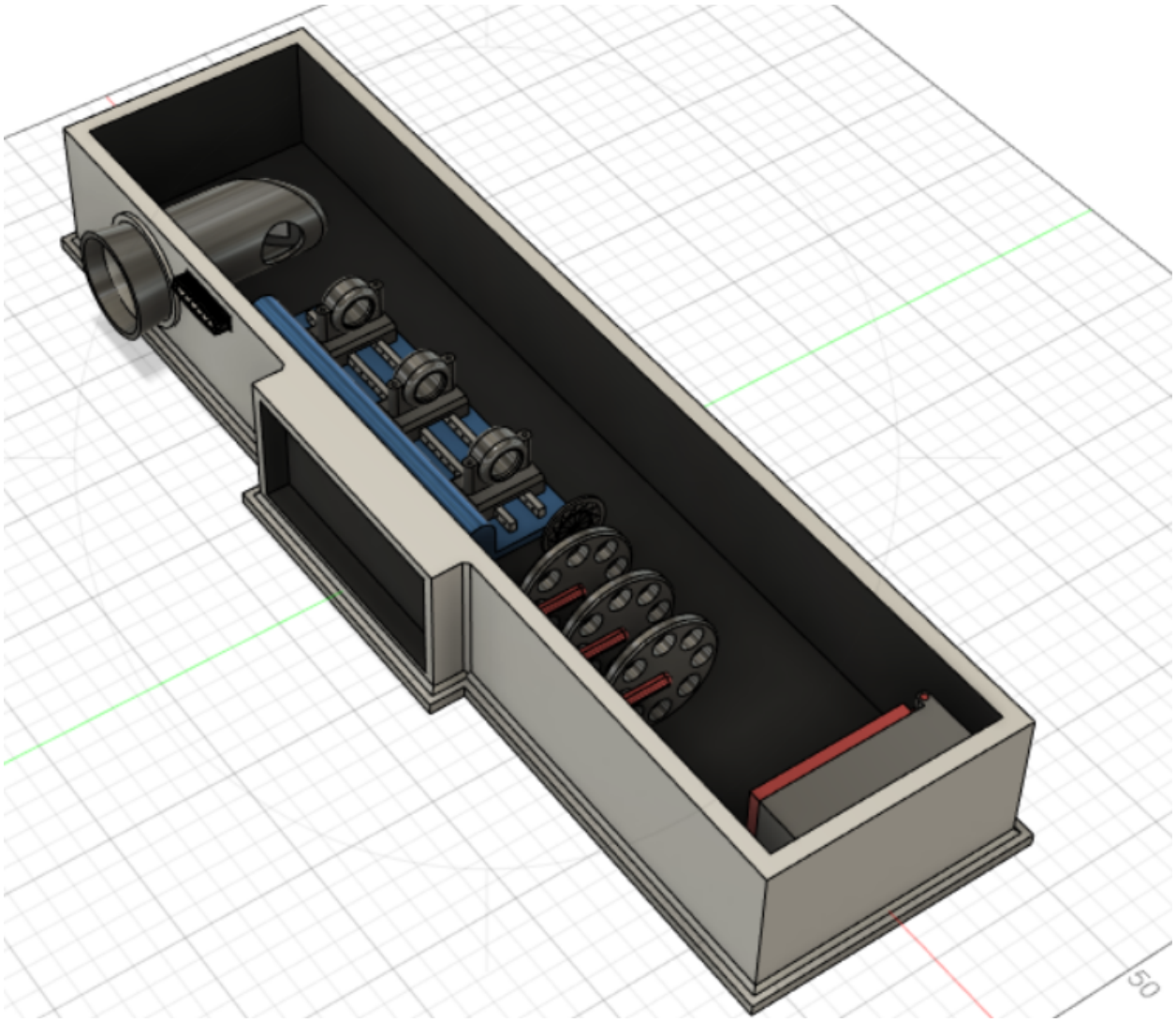

HOLOGRAPHIC SPECTROMETER

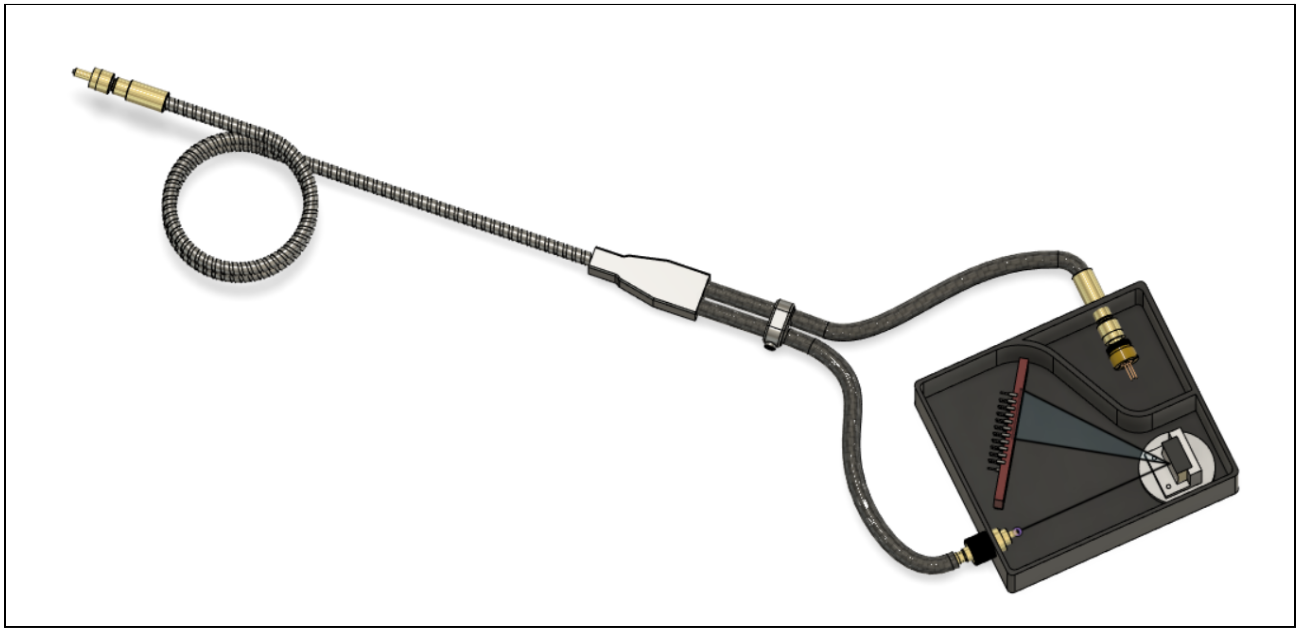

RAMAN SPECTROMETER

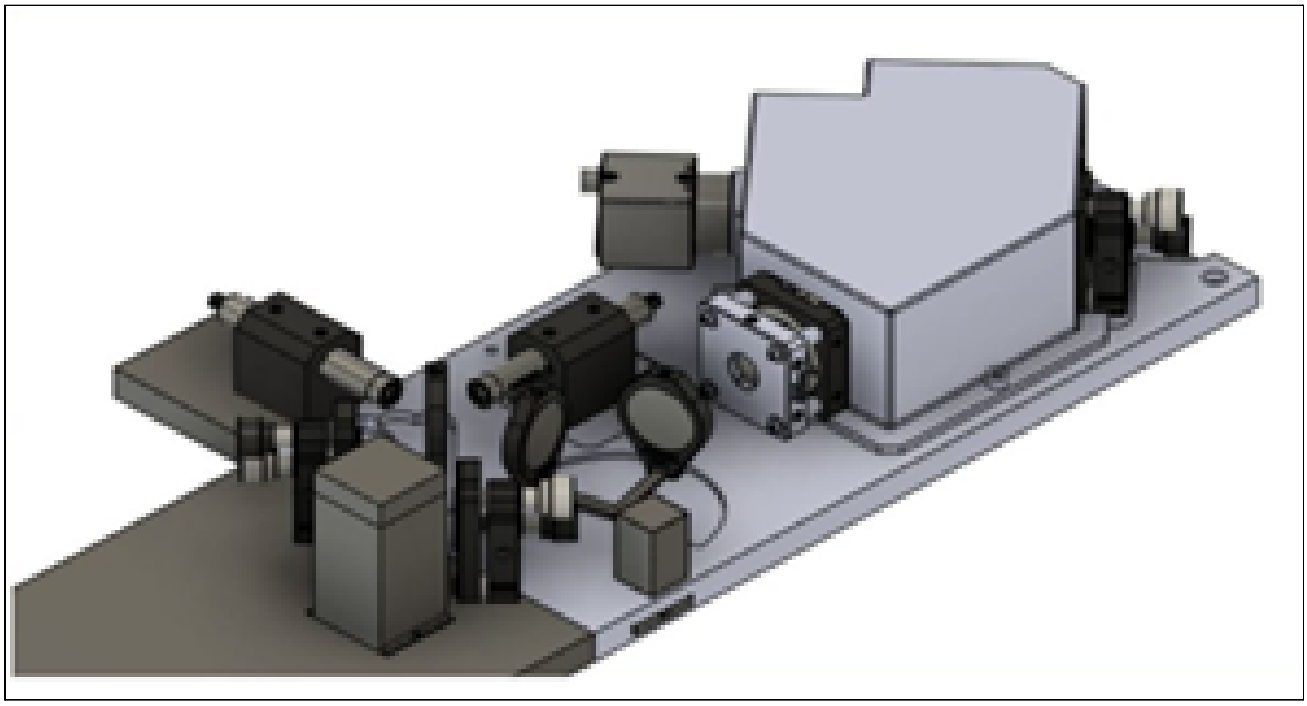

ALPHA-PARTICLE X-RAY SPECTROMETER

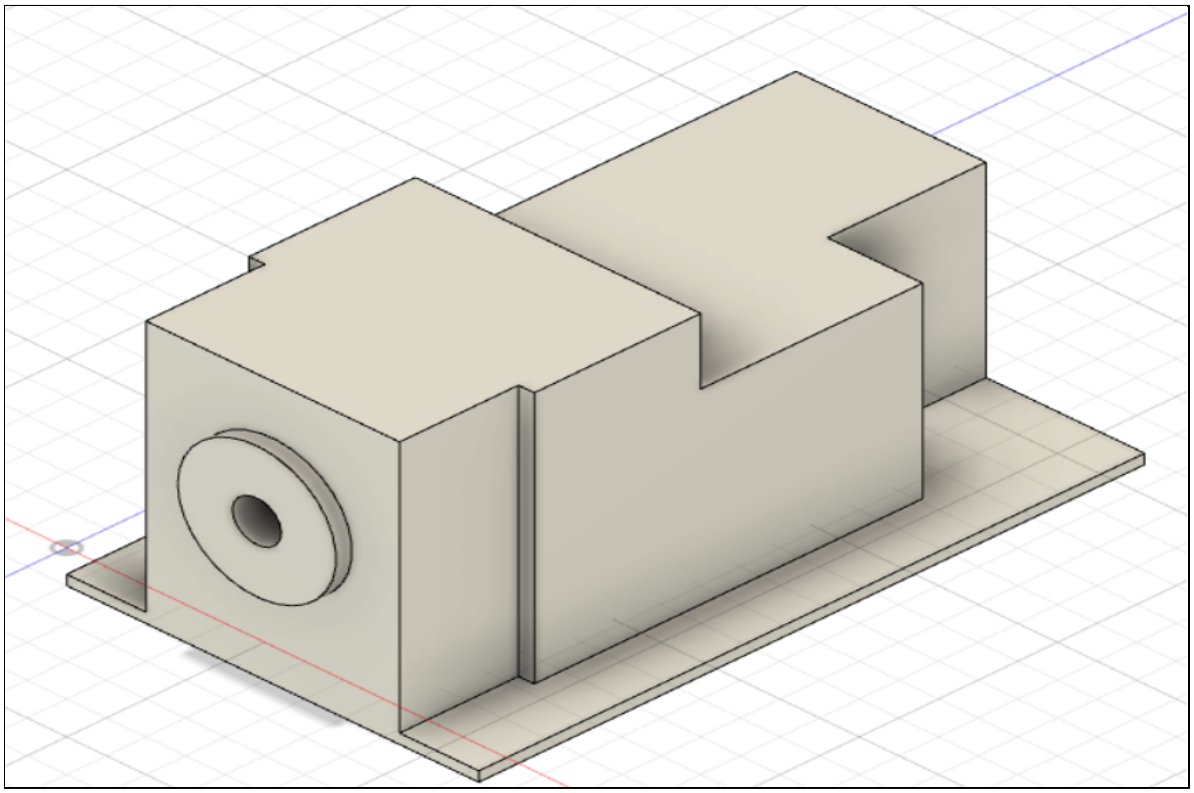

MINI - THERMAL EMISSION SPECTROMETER

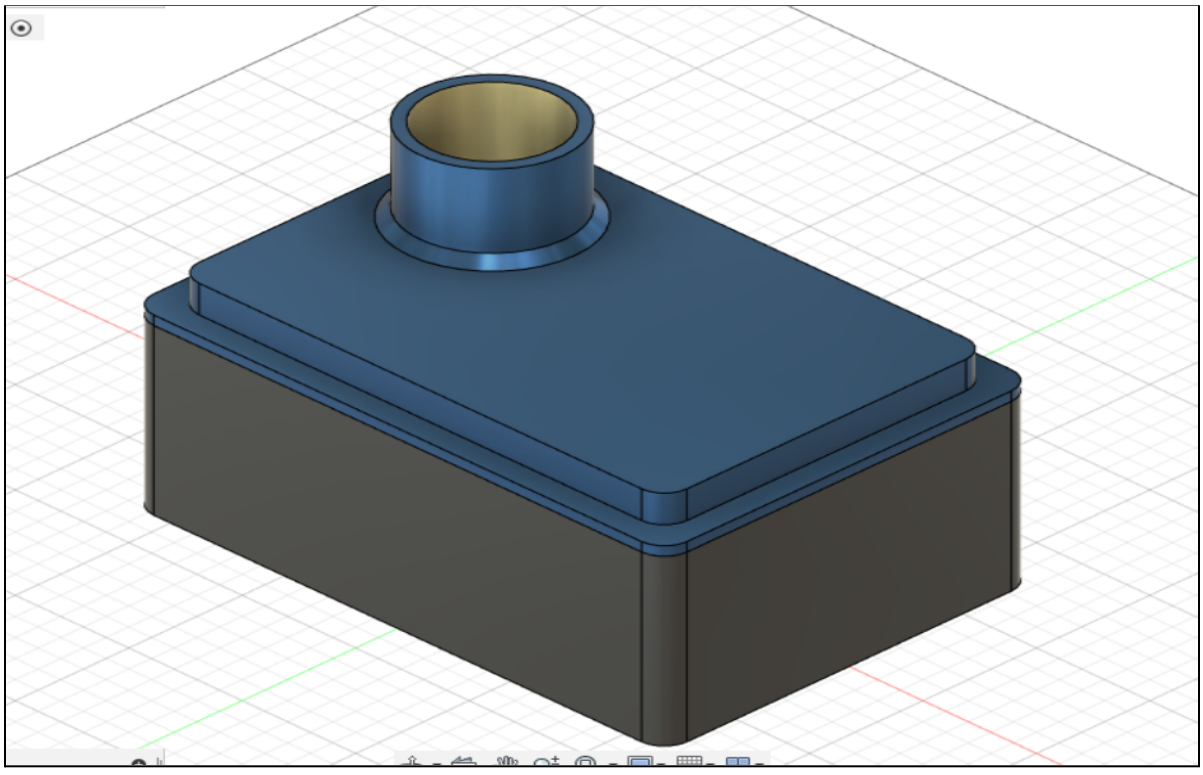

GROUND PENETRATING RADAR